"ANALYTICAL STUDY OF COLUMN FAILURE DUE TO BLAST LOADING"

A Thesis

Submitted in partial fulfillment of the requirements for the award of the degree of

MASTER OF TECHNOLOGY

IN

CIVIL ENGINEERING

With specialization in

STRUCTURAL ENGINEERING

Under the supervision of

Mr. Anil Kumar
(Assistant Professor)

By

Vijay Kumar
(142653)

to

JAYPEE UNIVERSITY OF INFORMATION TECHNOLOGY

WAKNAGHAT, SOLAN – 173 234

HIMACHAL PRADESH, INDIA

June, 2016

CERTIFICATE

This is to certify that the work which is being presented in the thesis titled **"Analytical study of Column Failure due to Blast Loading"** in partial fulfillment of the requirements for the award of the degree of Master of Technology in Civil Engineering with specialization in "**Structural Engineering**" and submitted to the Department of Civil Engineering, Jaypee University of Information Technology, Waknaghat is an authentic record of work carried out by **Vijay Kumar** (Enrolment No. 142653) during the period from July 2015 to June 2016 under the supervision of **Mr. Anil Kumar**, Assistant Professor, Department of Civil Engineering, Jaypee University of Information Technology, Waknaghat.

The above statement made is correct to the best of our knowledge.

Date: - ………………………

Dr. Ashok Kumar Gupta	Anil Kumar	External Examiner
Professor & Head	Assistant Professor	
Department of Civil Engineering	Department of Civil Engineering	
JUIT Waknaghat	JUIT Waknaghat	

ACKNOWLEDGEMENTS

Foremost, I would like to express my sincere gratitude to my advisor **Mr. Anil Kumar** for the continuous support of my thesis study, for his patience, motivation, enthusiasm, and immense knowledge. His guidance has helped me in all the time of this study and writing of this report. I could not have imagined having a better advisor and mentor for my thesis study. I would also like to thank him for lending me his precious time when I had went to him.

My special thanks are due to **Prof. Ashok Kumar Gupta,** Head of the Civil Engineering Department, for all the facilities provided.

I am also very thankful to all the faculty members of the department, for their constant encouragement during the project.

I also take the opportunity to thank all my friends who have directly or indirectly helped me in my project work.

Last but not the least I would like to thank my parents, who taught me the value of hard work by their own example.

Date: **Vijay Kumar**

ABSTRACT

The study of blast effects on structures has been an area of formal technical investigation for over 60 years. Over the past decade, the world has witnessed unprecedented levels of devastation from both natural disasters and terrorist attacks. Loss of life and injuries to occupants can result from many causes, including direct blast-effects, structural collapse, debris impact, fire, and smoke. The indirect effects can combine to inhibit or prevent timely evacuation, thereby contributing to additional causalities. In addition, major catastrophes resulting from gas-chemical explosions result in large dynamic loads, greater than the original design loads, of many structures. Due to such impacts of large dynamic loading, efforts have been made during the past few decades to develop methods of structural analysis and design of blast resistance structure. Since blast resistant design is the important topic of study and therefore requires the careful understanding about the blast phenomena and its effect and impact on various structural elements. Columns in a building are vital structural elements which resist lateral loads during earthquakes therefor, they should be robust enough to resist blast loads since failure of even a few columns may initiate progressive collapse of a building. In the present report, a column from a steel-moment-framed building is subjected to blast loading scenarios for blasts occurring outside the building and at ground level. The explosive material, trinitrotoluene (TNT) is placed at various locations with variable charge weight and standoff distance. The selected column is modeled in ANSYS-Autodyn® maintaining its fixity and axial loads as in the main building. Response of the column is captured for different blast scenarios. Peak Reflected Pressure is calculated manually by Kinney and Graham approach and is compared with that obtained from Autodyn. A comparative study has been presented for different types of column sections subjected to blast loads due to different TNT weights and standoff distances. The findings are helpful in predicting the progressive failure of the building and also in deciding the orientation of columns in a building.

CONTENTS

Chapter no.	*Description*	*Page no.*
	CERTIFICATE	i
	ACKNOWLEDGEMENTS	ii
	ABSTRACT	iii
	CONTENTS	iv-v
	LIST OF FIGURES	vi
	LIST OF TABLES	vii
1.	**INTRODUCTION**	**1-9**
	1.1 General	1
	1.2 Blast and Shock Phenomena	2
	1.3 Propagation in Free Air	4
	1.4 Chemistry of Explosives	7
	1.4.1 Oxidation	7
2.	**LITERATURE REVIEW AND OBJECTIVES**	**10-16**
	2.1 Literature Review	10
	2.2 Objectives of the study	16
	2.3 Need of the Project	16
3.	**METHODOLOGY**	**17-20**
	3.1 Computation of Blast Pressure	17
	3.1.1 Scaled Distance	17
	3.1.2 Peak Incident Pressure	17
	3.1.3 Positive time duration	18
	3.1.4 Positive Impulse	19
	3.1.5 Peak Reflected Pressure	19
	3.2 Numerical Modeling of building and column using ANSYS	20
4.	**COMPARISION OF BLAST PRESSURES**	**21-40**
	4.1 Problem Definition	21
	4.2 Peak Reflected Pressure Calculations (Kinney-Graham Approach)	22
	4.3 Calculation of Blast Pressure in ANSYS	31
	4.3.1 Modeling of building in ANSYS	31
	4.4 AUTODYN analysis of Building subjected to Blast Loading	34

Chapter no.	Description	Page no.
	4.4.1 Introduction to Autodyn	34
	4.4.2 Equation of State	34
	4.4.3 JWL equation of state	34
	4.4.4.Procedure	35
	4.5 Peak Reflected Pressure in Autodyn	38
	4.6 Conclusion drawn from both the Results	40
5.	**COMPARATIVE STUDY OF DIFFERENT COLUMN SECTIONS**	**41-61**
	5.1 General	41
	5.2 Results of Analysis	41
	5.3 Graphical Results	44
	5.3.1 Variation of Pressure with Time at different TNT weights for different sections	44
	5.3.2 Observations made from the above results	48
	5.3.3 Kinetic Energy for different Standoff Distances and TNT weights for different sections	49
	5.3.4 Conclusions drawn from above observations	50
	5.3.5 Variation of Different Parameters for different TNT weights and Stand-off Distances for I-section	51
	5.3.6 Conclusions drawn from above Plots	54
	5.3.7 Comparison of various properties of different column section	55
	5.3.8 Observations made from the comparison in above cases	61
6.	**CONCLUSIONS AND FUTURE SCOPE**	**62-63**
	6.1 Conclusions	62
	6.2 Future scope	63
	REFERENCES	**64-65**

LIST OF FIGURES

Figure no.	*Description*	*Page no.*
1.1	Pressure - Time History	3
1.2	Schematic of Blast Load	5
1.3	Blast wave Propagation	6
3.1	Reflected Pressure Coefficients	20
4.1	3D view of building used for Modelling	21
4.2	Front face of Building showing various parameters	23
4.3	UFC 3-340-02 (2008) Graphs discretized a) From 34.7 MPa to 0.34 MPa b) From 1.03 Mpa to 0.0014 MPa	24
4.4	Generation of points	31
4.5	Joining of points with lines	31
4.6	Cross-section allotment to beams and columns	32
4.7	Slab generation	32
4.8	Meshing of building	32
4.9	Application of loads	32
4.10	Workbench Layout	32
4.11	Air Medium surrounding Building	36
4.12	Gauge Points	36
4.13	Blast point in front of building	37
4.14	Blast waves	37
5.1	Deformation in Rectangular box section and Channel section	41
5.2	(a) Column and detonation point, (b) Gauge points for response computation	42
5.3	(a) Pressure contours in air around column, (b) Peak pressure-time history on column	42
5.4	(a) Blast pressure on column, (b) principal strain contours, and (c) Principal stress contours due to blast load at 1.47 ms.	43
5.5	Deformed column due to blast	43
5.6	Pressure vs Time for I-section	43

Figure no.	*Description*	*Page no.*
5.7	Pressure vs Time for R. B. section	45
5.8	Pressure vs Time for Channel section	46
5.9	Pressure vs Time for Circular section	47
5.10	Kinetic Energy for I-section	49
5.11	Kinetic Energy for R.B. section	49
5.12	Kinetic Energy for Circular section	50
5.13	Kinetic Energy for channel section	50

LIST OF TABLES

Table no.	*Description*	*Page no.*
4.1	Radial Distance & angle of incidence for stand-off distance 5m	25
4.2	Radial Distance & angle of incidence for stand-off distance 10m	26
4.3	Peak Reflected Pressure for TNT weight 50kg & 5m S.D.	27
4.4	Peak Reflected Pressure for TNT weight 100kg & 5m S.D.	28
4.5	Peak Reflected Pressure for TNT weight 50kg & 10m S.D.	29
4.6	Peak Reflected Pressure for TNT weight 100kg & 10m S.D.	30
4.7	Peak Reflected Pressure on gauge Points in Building for 50kg TNT	38
4.8	Peak Reflected Pressure on gauge Points in Building for 100kg TNT	39

CHAPTER 1

INTRODUCTION

1.1 General

The study of blast effects on structures has been an area of formal technical investigation for over 60 years. Over the past decade, the world has witnessed unprecedented levels of devastation from both Natural disasters and terrorist attacks. Extreme loading conditions generated by blasts that result from terrorist attacks can cause devastating consequences for structures and their occupants. The use of vehicle bombs to attack city centers has been a feature of campaigns by terrorist organizations around the world. A bomb explosion within or immediately nearby a building can cause catastrophic damage on the building's external and internal structural frames. It includes collapsing of walls, blowing out of large expanses of windows, and shutting down of critical life-safety systems. Loss of life and injuries to occupants can result from many causes, including direct blast-effects, structural collapse, debris impact, fire, and smoke. The indirect effects can combine to inhibit or prevent timely evacuation, thereby contributing to additional casualities. In addition, major catastrophes resulting from gas-chemical explosions result in large dynamic loads, greater than the original design loads, of many structures.

Disasters such as the terrorist bombings of the U.S. embassies in Nairobi, Kenya and Dares Salaam, Tanzania in 1998, the Khobar Towers military attacks in Dhahran, Saudi Arabia in 1996, the Murrah Federal Building in Oklahoma City in 1995, and the World Trade Centre in New York in 1993 have demonstrated the need for a thorough examination of the behaviour of columns subjected to blast loads.

Blast is a destructive wave of highly compressed air spreading outwards from an explosion.

An **explosion** is a very fast chemical reaction producing transient air pressure waves called blast waves. For a ground-level explosive device (such as a bomb in a vehicle), the pressure wave will travel away from the source in the form of a hemispherical wave-front if there are no obstructions in its path). The peak overpressure (the pressure above normal atmospheric pressure) and the duration of the overpressure vary with distance from the device. The magnitude of these parameters also depends on the explosive materials from which the bomb is made and the packaging method for the bomb. Usually the size of the bomb is given in terms of a weight of

TNT. City streets confine the blast wave and prevent it from radiating hemi spherically and this tends to increase the pressures to which buildings are subjected .The blast pressure waves will also be reflected and refracted by buildings, travelling around the corners and curves of a building. Blast waves are very intrusive: they will travel down side streets and over the tops of buildings, and thus all sides of a building will be subject to overpressures. As the wave moves further from the source of the explosion, the peak overpressure drops. However, the confining effect of buildings, called 'funneling', and rising ground means that the pressure drops more slowly than in open ground and buildings can be at risk at what might normally be considered safe distances.

When blast waves impinge directly onto the face of a building, they are reflected from the building. The effective pressure applied to that face of the building is magnified when this occurs. If a bomb is very close to a building, the building will also be impacted by shrapnel from the bomb packaging and by debris from the break-up of 'street furniture' such as litter bins and so on. This shrapnel moves at high velocity and will penetrate thin building facades and unprotected glazing. This effect will be hazardous to personnel who should, if possible, have the chance to avail themselves of the protection offered by solid internal walls.

1.2 Blast and Shock Phenomena

The shock wave which propagates through air as a consequence of an explosion is known as a **blast wave**.

The head of the blast wave, called the **shock front**, causes an abrupt rise in both overpressure and dynamic pressure as it passes a point as illustrated in figure 1.1. In the case of overpressure, this abrupt rise is followed by a decline to a pressure below ambient and then a gradual return to ambient. The portion of the wave in which the overpressure is above ambient is termed the positive over-pressure phase, while the remaining portion, where the pressure is below ambient, is called the negative pressure phase. The decrease in pressure below ambient in the negative phase is usually small in comparison with the increase in pressure in the positive phase. The blast wave front reaches at a given location at time t_A, and after the rise to the peak value, P_{so} the incident pressure decreases to the ambient value. The time taken is known as the positive phase duration. This is followed by a negative phase with duration to that is usually much longer than the positive phase. It is classified as a negative pressure below ambient pressure having peak magnitude of P_{so}^-. It occurs along turbulence of the particle flow. The negative phase has less significance in a design than is the positive phase, and its amplitude P_s^- must be less than ambient atmospheric pressure P_o. The incident impulse density related with the blast wave is the integrated area under the pressure time curve. It is described as i_s for the positive phase and i_s^- for the negative phase.

The dynamic pressure associated with mass motion of air has a positive duration somewhat greater than the overpressure positive duration. During this period the transient winds blow in the direction of shock motion. The wind velocity after decreasing to zero reverses direction of nuclear explosion. The dynamic pressure associated with this reverse flow is insignificant.

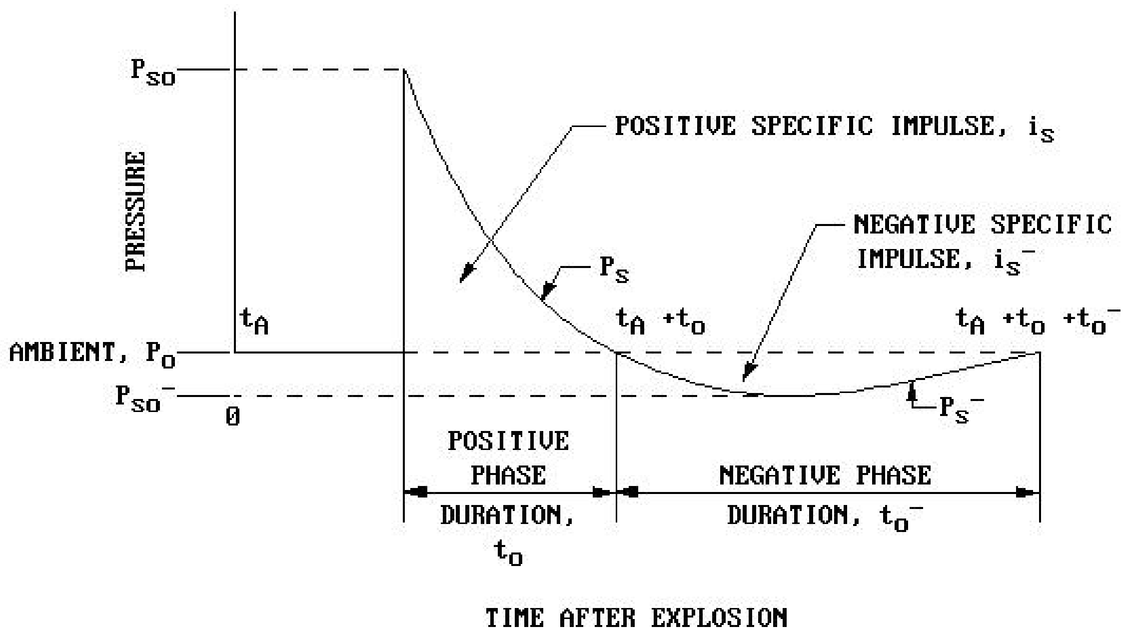

Fig. 1.1 Pressure-Time History

1.3 Propagation in Free Air

a) General:- As the blast wave moves out from the fireball region, various changes in its physical characteristics occur as a function of time and distance. In free air, i.e., in a homogeneous atmosphere where no boundaries or surfaces are present, these changes take place in a definite manner as a result of spherical divergence and irreversible energy losses to the air through which the blast wave propagates. The shock front velocity and peak over-pressure decrease with increasing distance, while the duration of the positive phase increases. Other blast wave parameters are affected in a similar way, so that the blast wave is said to be attenuated with distance.

b) Time of arrival:- As the shock front travels away from an explosion under sea level conditions, its velocity of propagation at breakaway is approximately seven times the velocity of sound. As the peak overpressure approaches zero, however, the shock front velocity approximates sonic velocity.

c) Overpressure:-

(i) **Peak overpressure**:- The term over-pressure, expressed in pounds per square inch (psi), is used to describe an increase in pressure over ambient. Peak overpressure is the highest over-pressure reached during the passage of the blast wave.

(ii) **Duration:-** The duration of the positive overpressure phase of a blast wave from a nuclear detonation of a given yield increases as the peak overpressure decreases with distance. Also the duration of the positive overpressure phase for a given peak overpressure increases as the yield increases.

(iii) **Impulse and wave forms:-** In many cases, the damage resulting from a nuclear detonation is more nearly a function of both the positive phase overpressure and its duration, specifically the over-pressure impulse, than upon peak over-pressure alone. The overpressure impulse (I,) of the positive phase of the blast wave is the area under the positive portion of the overpressure-time curve as illustrated in figure 1.1. This curve or wave form varies in an exponential fashion, depending on the peak overpressure. Negative phase impulse is similarly defined in terms of the under-pressure; however, it is usually less significant than the positive phase impulse.

d) Dynamic pressure:- A wind of high velocity blowing in the direction of shock motion exists immediately behind the shock front. Dynamic pressures are a measure of the drag forces associated with these winds and are a function of the density and particle velocity of the air behind the front. Dynamic pressure is denoted by 'q' and is expressed in pound per square inch. The wind velocities following the shock front exist only for short periods and diminish as blast wave over-pressure decreases.

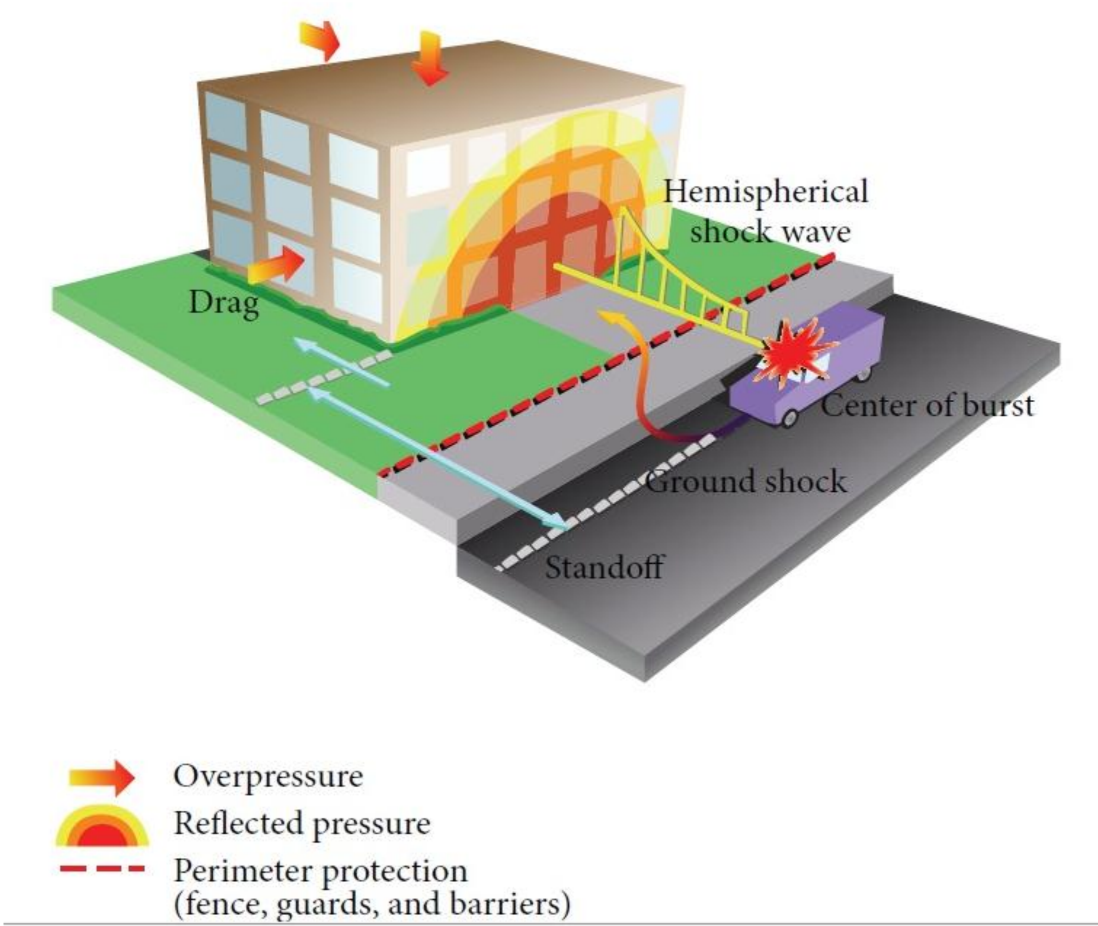

Fig. 1.2 Schematic of Blast Load

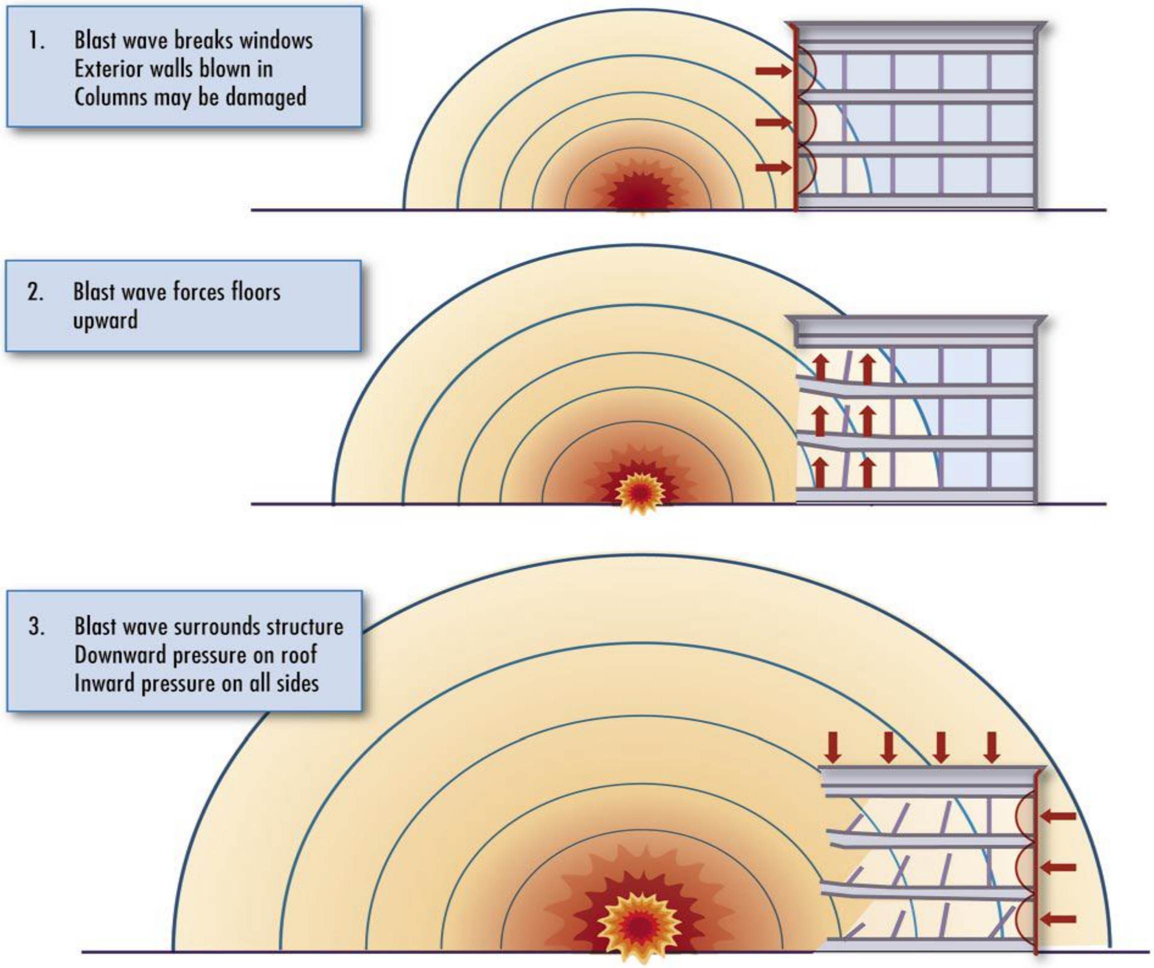

Fig. 1.3 Blast wave Propagation

<u>As per IS 4991 1968</u>, "Indian Standard CRITERIA FOR BLAST RESISTANT DESIGN OF STRUCTURES FOR EXPLOSIONS ABOVE GROUND" , Structures designed to resist blast loads are subjected to completely different type of load than that considered in conventional design. Here they are hit with a rapidly moving shock wave which may exert pressures many times greater than those experienced under the greatest of hurricanes. However, in blast phenomenon, the peak intensity lasts for a very small duration only. The blast wave loads the exposed surface of the structure and then the load is transmitted to the other elements. Thus, the response of each individual element is important unlike the ground motion wherein the whole structural system is simultaneously causing inertia effects on all parts.

To design a structure capable of resisting these intense but short duration loads, members and joints are permitted to deflect and strain much greater than is allowed for usual static loads. This permitted deflection is, ordinarily, well into the plastic range of the material. Large amounts of energy are absorbed during this action, thus reducing the required design strength considerably below that required by conventional design within elastic range. Moreover, under higher rates of loading the strength developed by the material, increases with the rate of loading, and may often be adequately described as a function of time within a certain range.

Strategies for blast protection have become an important consideration for structural designers as global terrorist attacks continue at an alarming rate. Conventional structures normally are not designed to resist blast loads and because the magnitudes of design loads are significantly lower than those produced by most explosions, conventional structures are susceptible to damage from explosions. No civilian buildings can be designed to withstand the kind of extreme attack that happened to the World Trade Centre in USA. Building owners and design professionals alike, however, can take steps to better understand the potential threats and protect the occupants and assets in an uncertain environment. With this in mind, developers, architects and engineers increasingly are seeking solutions for potential blast situations, to protect building occupants and the structures.

1.4 Chemistry of Explosives

Modelling and Analysis of explosive detonations requires a good understanding of chemistry because the chemical composition of an explosive source governs its physical properties like detonation velocity. Explosive detonations are products of complex physical and chemical processes within and in the immediate vicinity of the explosive and are accompanied by a near-instantaneous release of a huge amount of energy in the form of heat, light and sound. The chemical reactions involved in a detonation are thus oxidation and exothermic reactions because the reactants are oxidized to give a mixture of hot gaseous products.

1.4.1 Oxidation

There are two major types of oxidation reactions involved in a detonation.

- In the first type, there are two reactants, a fuel and an oxidizer, that react to form the products of the explosion.

- The second type of reaction, involves a single reactant where the fuel and the oxidizer are contained in the same molecule, which decomposes during the reaction and is transformed into oxidized products. It is more common in explosives.

The majority of the explosives consist of single molecules made up of Carbon (C), Hydrogen (H), Nitrogen (N) and Oxygen (O). These are called CHNO explosives and can be represented by the general formula $C_cH_hN_nO_o$, where *c*, *h*, *n*, *o* are the number of carbon, hydrogen, nitrogen and oxygen atoms, respectively, contained in one molecule of the explosive. During the decomposition2 reaction, the reactant molecule breaks down into its individual component atoms as follows

$$C_cH_hN_nO_o, \rightarrow cC + h\,H + nN + oO$$

These individual atoms then recombine to form the final products of the reaction. The order of reaction is

$$2N \rightarrow N_2$$

$$2H + O \rightarrow H_2O$$

$$C + O \rightarrow CO$$

$$CO + O \rightarrow CO_2$$

If oxygen remains after the formation of carbon dioxide, then the explosive is called over-oxidized. Any oxygen left after the formation of CO_2 forms O_2. However most explosives, with the exception of nitro-glycerin and ammonium nitrate, do not have sufficient oxygen to convert all of the carbon to CO_2 and these are called under-oxidized explosives. For such explosives, the products of the reaction extract oxygen from the surrounding air as they expand freely. While doing so, these products mix with oxygen and may burn to form CO_2. These secondary reactions are part of a process known as afterburning.

The relative amount of oxygen in an explosive is therefore an important factor in determining the nature and reactivity of the detonation products; it is quantitatively expressed as oxygen balance. The heat generated by an oxygen-deficient explosive (such as trinitrotoluene (TNT)) is less than that generated by an explosive that oxidizes completely.

“The Column” in a building is the most important load carrying element through which the load is transferred to the foundation. If the column is not able to withstand the load, then the whole building will get collapsed in not time. Column is a compressive load carrying member on which the load from the beams came and it transfers the load to the foundation. Depending upon various physical and environmental conditions, the columns may also be designed to resist lateral loads coming on the building.

In steel frame structures, the damage and failure of a structural column from a blast load can result in a progressive collapse and catastrophic failure of the entire structure. The objectives of this study is to develop experimental methodologies, analysis strategies and threat assessment tools that can be used to mitigate blast hazards and predict damage in structural steel frame structures. Typically, guidelines and methodologies are developed from conclusions drawn via field testing with live explosives, but due to the harsh environment created by explosives, collecting reliable data is problematic.

When a column is subjected to lateral load due to blast pressure, the static compressive axial load acting on the column affects the dynamic response of the column. The blast load induces lateral deformation in the column, which causes the applied and resisting axial forces to form a couple as they are no longer collinear. The couple causes additional lateral deformation and bending in the column. This is known as P-δ effect, which tends to magnify the primary bending moment due to blast pressure and reduces the column

Load carrying capacity. The column subjected to blast loading, results in secondary moments that diminish its pure moment resistance.

So when a building is subjected to blast loading, its different members are subjected to the Peak incident and reflected pressures due to blast. The intensity of pressure will be more in the members nearer to the point of blast and vice-versa. The pressure due to blast will first increase and then decrease after few seconds of blast. So the objective is to study and analyze the behaviour of building and columns due to blast loading. The Peak Reflected pressure at various grid points that will be generated by blast in Autodyn ANSYS is to be compared with the one to be computed by Kinney-Graham Approach. Different column sections are to be analyzed in Autodyn and various results are to be compared at various standoff distances and charge weights.

CHAPTER 2

LITERATURE REVIEW AND OBJECTIVES

2.1 Literature Review

Dewey (1971) studied “The properties of the blast waves obtained from the particle trajectories”. First time he introduced the effect of spherical and hemispherical TNT (trinitrotoluene) in blast waves and determined the density throughout the flow by application of the Lagrangian conservation of mass equation which used for calculating the pressure by assuming the adiabatic flow for each air element between the shock fronts. The temperature and the sound speed found from the pressure and density, assuming the perfect gas equation of states.

Dharaneepathy (1995) studied “The effects of the stand-off distance on tall shells of different heights” carried out with a view to study the effect of distance (ground-zero distance) of charge on the blast response. An important task in blast-resistant design is to make a realistic prediction of the blast pressures. The distance of explosion from the structure is an important datum, governing the magnitude and duration of the blast loads. The distance, known as ‘critical ground-zero distance’, at which the blast response is a maximum. This critical distance should be used as design distance, instead of any other arbitrary distance.

Remennikov (2003) studied “The methods for predicting bomb blast effects on buildings”. When a single building is subjected to blast loading produced by the detonation of high explosive device. Simplified analytical techniques used for obtaining conservative estimates of the blast effects on buildings. Numerical techniques including Lagrangian, Eulerian, Euler- FCT, ALE, and finite element modeling used for accurate prediction of blast loads on commercial and public buildings.

Khadid et al. (2006) studied “The fully fixed stiffened plates under the effect of blast loads” to determine the dynamic response of the plates with different stiffener configurations and considered the effect of mesh density, time duration and strain rate sensitivity. He used the finite element method and the central difference method for the time integration of the nonlinear equations of motion to obtain numerical solutions.

Ronald L. Shope (2006) studied "The response of wide flange steel columns subjected to constant axial load and lateral blast load". The finite element program ABAQUS was used to model with different slenderness ratio and boundary conditions. Non-uniform blast loads were considered. Changes in displacement time histories and plastic hinge formations resulting from varying the axial load were examined.

Mark et al (2006) studied "A Model of Progressive Collapse of conventional framed building" and provides efficient alternative to dynamic analysis of a moment-framed building subjected to blast loading or blast induced damage. The circles and column are designed to withstand factored dead and lives load. Structural damage due to blast loading includes local plastic hinge formation, member failures from area stress, local buckling and global buckling. The modal considers yield of failures events at hinged beam element and stability of structure according to US buildings code requirements. This approach provides an efficient modal that auto makes a non-linear static analysis of a damaged building for its purpose of predicting progressive collapse.

Vlassis et al (2006) published "Progressive collapse of multi-storey buildings due to sudden column Loss" presents a principle of a new design oriented methodology for progressive collapse assessment of multi-story building .This paper deals with the study of sudden removal of peripheral column and corner column. Such structures are prone to progressive collapse due to failure of internal secondary beam support points. Despite satisfying codal provisions, bare steel beams were unable to survive column removal. The susceptibility of progressive collapse is mainly related to the beam span sizes, which are required to safely transfer the applied gravity load to the undamaged structure. The fin plates which are used for beam to beam points of internal secondary beam are less adequate then flexible end plates due to increase flexibility and reduce strength. But as they are ductile, so their use in robustness design should be carefully reviewed.

Ngo et al. (2007) for their study on "Blast loading and Blast Effects on Structures" gives an overview on the analysis and design of structures subjected to blast loads phenomenon for understanding the blast loads and dynamic response of various structural elements. This study helps for the design consideration against extreme events such as bomb blast, high velocity impacts.

Young and James (2008) in "Response of a low rise steel building to air blast" suggested that building will have greater resistance to blast loads if it is designed for strong ground motion. Three storey steel building is modelled and magnitude and distribution of blast load using computer software is estimated. For generating air blast loading, hemispherical surface of different weight and at different distance is considered. A standoff distance of greater than 15 feet should provide adequate protection against blast. Demand/capacity (D/C) ratio is used to indicate area of potential problem, when non-linear analysis is conducted. Rigid diaphragm is effective in distributing the blast load from the front fall to the other frame on the perimeter, provided that pressure does not enter to the building.

FengFu (2009) in "Progressive collapse analysis of high rise building with 3-D finite element modeling method" analyzed a 20-storey building which was modeled in ABAQUS to perform the progressive collapse analysis. On this model, overall behavior of 20 storey buildings under the sudden loss of column is analyzed which will provide essential information on progressive collapse resisting design. The dynamic response of the structure is related to affect loading area after the removal of column from which we have an idea about the amount of energy need to be absorbed by the building. At column removal level, each member and beam to column connection should be designed for twice static axial force obtained after load combination. Column removal at higher level will induce larger vertical displacement than a column removal at lower level.

Wibowo and Lau (2009) in "seismic progressive collapse: qualitative point of view" said that progressive collapse occur because of human-made and nature hazards. Current focus is on preventing collapse due to abnormal gravity and blast loads. This paper presents insides and issues related to progressive collapse behavior of structure caused by earthquake loading. Earth quake loading can generate strong lateral fostrces and stress reversal. From past it can be shown that seismic loads can cause structural damage which results in loss of supports the structure. Linear static analysis is the fastest and easiest to perform earth quake force analysis but it is applicable for regular and simple configuration only. Linear dynamic analysis gives most exact result and is often used as a verification to supplement results from other methods.

Taewan et al. (2009) in " Investigation of Progressive Collapse-Resisting Capability of steel Moment Frames using Push Down Analysis " concluded that the load resisting capacity increased as the no. of storeys and the no. of spans increases but if the length of the span is increased, the load resisting capacity against progressive collapse decreases. These results when compared with incremental nonlinear dynamic analysis depicts that the maximum load factors resulted from the dynamic analysis were a little less than those from push down analysis. As the no. of bays and design earthquake load increases, the resistance to progressive collapse also increases.

Jinkoo et al (2010) in "Sensitivity analysis of steel buildings subjected to column loss" studied the sensitivity of design parameters such as yield strength of beams, column and braces live load elastic modulus and damping ratios of steel buildings subjected to progressive collapse. The different methods involved were Monte Carlo Simulation (MCS), Tornado Diagram Analysis (TDA) and First Order Second Moment Method (FOMS). The methods are applied to 3-storey, 10-storey and 20-storey buildings. One of the bottom storey columns were removed to initiates progressive collapse. The analysis shows that beam yield strength was most important parameter in moment resisting frame buildings and column yield strength in dual system building. Damping ratio was the most important parameter in dynamic analysis. The sensitivity study shows that the lower storey beams play more important role in resisting progressive collapse than upper story beams.

Peirs et al (2011) in their paper "Determining the stress strain behaviour at large strains from high strain rate tensile and shear experiments." said that to characterize the high strain rate mechanical behaviour of metals, Split Hopkinson Bar experiments are frequently used. These experiments tells the force and elongation history of specimen which can tell us about material structure behaviour. A combined experimental-numerical approach is use to extract the strain rate and temperature developed material behaviour. The stress strain behaviour of Ti-6A1-4V is determined by using both high strain rate in plane shear and tensile test results. The material behaviour is modeled with Johnson Cook constitutive relation. It is concluded that the Ti-6A1-4V exhibit more strain hardening shear than in tensile while the fractured strain in shear is lower than the tensile loading. The simultaneous use of tensile and shear test to identify the model parameters gives more generally applicable model.

Mehrdad et al.(2011) published a paper regarding Progressive collapse Resistance of an Actual 11- Storey Structure Subjected to severe Initial Damage. This paper investigates progressive collapse resistance of the Crowne Plaza Hotel, an 11-story aboveground structure in Houston, Texas, that was constructed in 1973. The experimental study depicts that the initial damage was caused by simultaneous explosion of four first floor neighbouring columns and two second floor perimeter deep beam segments. The structure resisted progressive collapse with a maximum permanent vertical displacement at the top of the exploded columns of only about 56 mm. The progressive collapse resistance of the structure is significantly affected by the axial compressive force developing in beam. The beam axial compressive force enhances its flexural strength and in turns its resistance to progressive collapse. Two analytical models were developed out of which one includes only flexural degrees of freedom and other includes both flexural and axial deformations.

Stefan and Ted (2012) studied the “Energy flow in Progressive collapse of steel framed buildings” and concluded that a building can arrest the collapse and achieve its stable configuration only if its K.E. is completely dissipated by the structure otherwise the remaining energy will cause the collapse to continue K.E. is dissipated in a structure by the transformation into their deformation energy. The sudden release of gravitational energy will always results in motions and K.E. A column that survives a collapse initiating event responds dynamically before eventually coming to rest. The deformation energy limit is helpful in the identification of column which experience transient instability, but do not fails. The structural members dampers the motions resulting from abnormal loadings. So for further studies, energy dissipated through it use of friction, fluid dampers metal based honey-comb devices dissipate energy should be given important.

Nassar et al (2012) in their research of "Strength and stability of Steel beam columns under blast load" used two models. First model was based on SDOF approximation and concept of equivalent lateral load was applied to simulate beam – column interaction. The second model was based on three dimensional FEM using LS-DYNA software. The result from SDOF analysis is compared with unified facilities criteria (UFC 3-340-02) design manual of structure. It is conclude that UFC over-estimates the column capacity for ductility ratios (meu) >1 irrespective of P/P_e ratio. Also for P/P_e>0.5 and meu<1, UFC still over estimates the actual column capacity. For such problem in actual, non-dimensional beam column curves are developed to include the effects of blast load and column properties on both its strength and stability.

Tavakoli and Kiakogouri (2013) in their study of "Influence of sudden Column loss on Dynamic Response of steel moment frames under blast Loading." invested the progressive failure using alternate load method and non – linear Dynamic analysis. They studied the structural response of building under sudden loss of column with or without external blast loading. Results shows that the progressive collapse is dependent on location of column loss. Non-linear dynamic analysis provides larger structural response than linear dynamic analysis. According to the results, the standoff distance is very sensitive in structural responses. So increasing distance with reduce the structural damage.

Xuemei and Jun (2013) had done their research work on " Validation of Johnson Cook Plasticity and Damage using impact Experiment". The dynamic behaviour of Ti-6A1-4V under high speed ball impact at various velocities and angles was assessed to validate Johnson Cook Constitutive relation. White- light scanning was performed to characterize impact craters formed on target surfaces. The measured crater was compared with those developed using finite element code ABACUS. The validation of J-C plasticity and damage model provides the basis for using this material model in simulation of other dynamic problems such as sand erosion behaviour of Ti-6A1-4V.

Brian and Halil (2013) in "Experimental and analytical progressive collapse assessment of a steal frame building" investigates the progressive collapse potential of an existing steel frame building by physically removing 4-first story column to understand the load redistribution within the building. Field test results are used to compare computational models and buildings. The 3-D models are more accurate than 2-D models as they are avoid overly conservative solutions and lower DCR value and vertical displacements. The shown values calculated from non-linear dynamic analysis are smaller than the linear static analysis and were closed for measure strains. This papers study reveals that it’s better to consider actual properties ad connections of the building to obtain reliable results.

Nassar et al (2014) in their paper “Dynamic Response of Steel Column subjected to blast Loading” studied the behavior of 13 wide – flange steel columns using live Explosive involving 50-250 kg of Ammonium nitrate/ fuel oil (ANFO) using field tests. The column carries axial loads equal to 25% of their axial load carrying capacity. Results shows that, the Axial load on column may increase the maximum lateral displacement of the column due to P-Delta effect and may decrease the lateral displacement by the elongation of the column fundamental period. In columns that experienced plastic deformation, the axial load can increase the maximum lateral deformation by up to 158%. The axial bending interaction increases the strain rate in the plastic range of the response by upto 93%.

2.2 Objectives of the Study

- To compute Peak Reflected Pressure using **Kinney-Graham Approach**.
- Comparative study of Peak Reflected Pressure from Kinney-Graham and that calculated from Autodyn ANSYS software.
- To compare the analysis results of various column sections.

2.3 Need of the Project

- As the terrorist attacks are increasing day by day, so it is necessary for the buildings to resist these effects produced from blast loads up to certain extent.
- The cylinder explosions in kitchens can also cause the catastrophic failure of buildings due to failure of column in that area.
- Due to sudden striking of vehicle like trucks due to unbalancing can also cause the ground floor columns to fail which can lead to progressive failure of the building.

CHAPTER 3

METHODOLOGY

3.1 Computation of Blast Pressure

3.1.1 Scaled Distance

All the Blast Pressure calculations are based on scaled distance as it is the important parameter in blast phenomena. It gives relation between Radial distance and charge weight. It is denoted by 'Z'. Mathematically,

$$\text{Scaled Distance (Z)} = \frac{R}{\sqrt[3]{W}} \qquad (3.1)$$

Where, *R* is the radial distance (in m) from the explosion and *W* is charge weight, generally expressed in pounds or kilograms.

3.1.2 Peak Incident Pressure

The sudden increased value of the pressure on the surface due to an explosion resulting at a distance from the surface parallel to the propagation of the blast wave is called as the peak incident pressure. In Literature, various empirical relations are available to determine the pressure on the surface when the blast waves are unimpeded in its motion.

Following relation for Peak Incident Pressure was given by Brode:

$$P_{pos} = \frac{6.7}{Z^3} + 1\,\text{bar} \ (P_{pos} > 10\text{bar}) \qquad (3.2)$$

$$P_{pos} = \frac{0.975}{Z} + \frac{1.455}{Z^2} + \frac{5.85}{Z^3} - 0.019 bar \ (0.1 < P_{pos} < 10 \text{ bar}) \qquad (3.3)$$

In 1961, Newmark introduced following relationship to calculate the maximum blast pressure (P_{SO}), in bars, for a high explosive charge detonates at the ground surface as:

$$P_{pos} = 6784\frac{W}{R^3} + 93(\frac{W}{R^3})^{1/2} \tag{3.4}$$

Mills introduces another expression of the peak overpressure in kPa, in which W is the equivalent charge weight in kilograms of TNT and Z is the scaled distance.

$$P_{pos} = \frac{1772}{Z^3} + \frac{114}{Z^2} + \frac{108}{Z} \tag{3.5}$$

In 1985, Kinney and Graham presented the following equation to compute the peak positive overpressure based on the analysis of large experimental data:

$$P_{POS} = P_O \frac{808\left[1+\left(\frac{Z}{4.5}\right)^2\right]}{\sqrt{\left[1+\left(\frac{Z}{0.048}\right)^2\right]} \times \sqrt{\left[1+\left(\frac{Z}{0.32}\right)^2\right]} \times \sqrt{\left[1+\left(\frac{Z}{1.35}\right)^2\right]}} \text{ (bar)} \tag{3.6}$$

3.1.3 Positive time duration (t_{pos})

The time difference between passing of a wave front and the end of the positive pressure phase marked by the passing of zero pressure point at a particular surface is called as the positive time duration (t_{pos}) of the blast wave. The positive time duration of a blast wave on any surface depends on the dissipation of the waves around that surface. If the surface is of small size, the positive time duration will be less as compared to a larger surface as the time required to surpass the surface will be more, hence, less dissipation possible.

Kinney and Graham (1985) presented the following relation for the positive time duration:

$$t_{pos} = W^{1/3} \frac{980\left[1+\left(\frac{Z}{0.45}\right)^{10}\right]}{\left[1+\left(\frac{Z}{0.02}\right)^3\right] \times \left[1+\left(\frac{Z}{0.74}\right)^6\right] \times \sqrt{\left[1+\left(\frac{Z}{6.9}\right)^2\right]}} \text{ (ms)} \tag{3.7}$$

3.1.4 Positive Impulse (I_{pos})

The area under the pressure-time history curve is called as impulse. The peak pressure decreases rapidly from the highest value to zero, described as quasi-exponential decrease. For simplicity, this decrease in the value of the peak pressure can be considered as triangular, rectangular keeping the impulse constant. The following are the empirical relations available for calculating the impulse of a wave pressure wave.

$$I_{pos} = \frac{0.067\sqrt{\left[1+\left(\frac{Z}{0.23}\right)^4\right]}}{Z^2\sqrt[3]{1+\left(\frac{Z}{1.55}\right)^2}} \text{ bar-ms} \qquad (3.8)$$

3.1.5 Peak Reflected Pressure (P_{ref})

When a pressure wave generated from an explosion impinge a surface at an angle, it is reflected, which results in higher pressure on the surface than the incident side-on pressure. The magnitude of the reflected pressure depends on the angle of incidence of the blast wave, the radial distance of the detonation point from the surface, peak incident pressure developed due to the explosion, the type of pressure wave, and the properties of the surface. The magnitude of the reflected pressure is generally determined from the coefficient of reflection,

$$P_{ref} = C_r P_{pos}$$

Where C_r = Coefficient of reflection.

UFC 3-340-02 gives the detailed procedure of determining the peak reflected pressure on a surface depending upon the peak incident pressure and angle of incidence of the waves. The coefficient of reflection (C_r) based on the peak incident pressure of the explosion and the angle of incidence of the blast wave at a particular point on the surface. The angle of incidence varies from 0° (wave parallel to the surface) to 90° (wave perpendicular to the surface) with the peak incident pressure as shown in figure below:

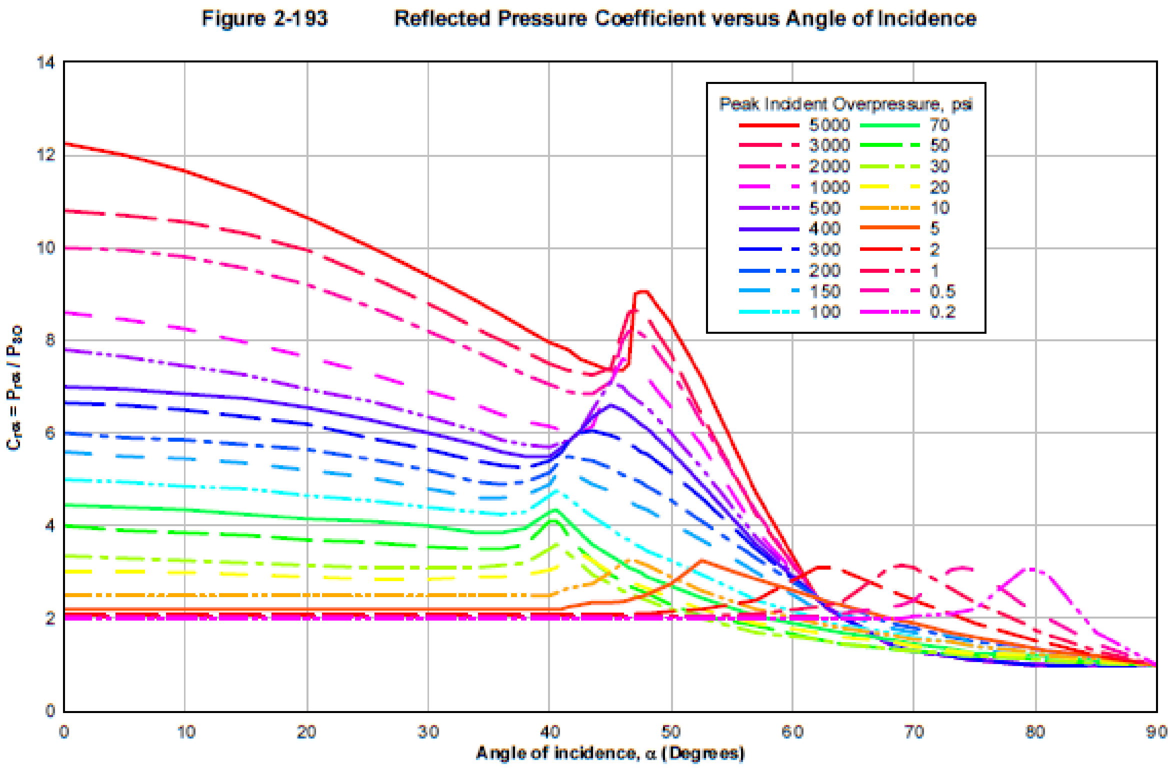

Fig 3.1 Reflected Pressure Coefficients

3.2 Numerical Modeling of building and column using ANSYS

The modeling of the building and application of blast pressure to Building is done by using ANSYS software. The Blast loading analysis is to be done in Autodyn.

CHAPTER 4

COMPARISION OF BLAST PRESSURES

4.1 Problem Definition

- This is a typical low rise steel building. All prevailing requirements for gravity, wind, and seismic design have been considered. It was designed for a typical office occupancy live load of 2.5 kPa.
- The floors were assumed to support a dead load of 4 kPa, which included a concrete-steel composite slab, steel decking, and ceilings/ flooring.
- This is a Three-storeyed steel - building which consists of 4-bays @ 9.15m along x-axis and 2-bays @ 9.15m along z - axis.
- The storey height is 3.96 meters.
- Slab thickness is taken as .125 meters.

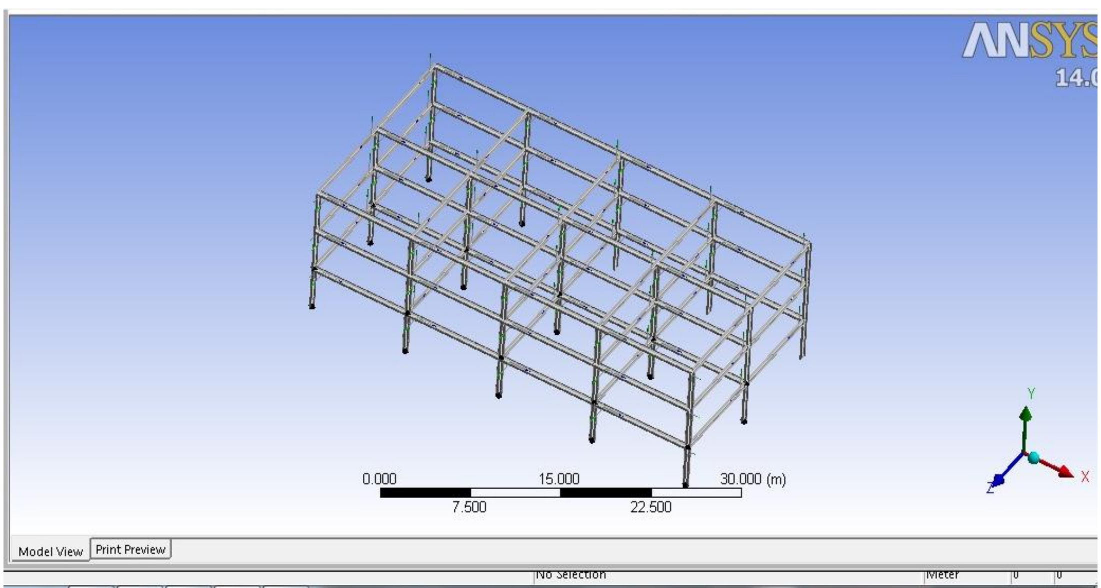

Fig. 4.1 3D view of building used for Modelling

4.2 Peak Reflected Pressure Calculations (Kinney-Graham Approach)

The Peak Reflected Pressure is calculated using Kinney and Graham Approach at the grid points. An excel program is made as the various parameters used to calculate pressure can be varied. eg. Stand-off distance and TNT weight.

For Calculating Peak Reflected Pressure as per Kinney-Graham Approach, following steps are followed:

1) First of all the values of radial distance and angle of incidence at various grid points for various standoff distances is calculated through a program in excel. Various parameters are shown diagrammatically in Fig. 4.2. The calculated data is attached in sheets.
2) After this the values of Peak Incident Pressure, Positive Impulse and positive time Duration is calculated from Kinney-Graham Approach at these grid points.
3) After calculating the value of Peak Incident Pressure and angle at various grid points, the value of coefficient of reflection is interpolated from the graphs in UFC 340-3-2 for various values of Peak Incident Pressure and at various angles. The record of the same is attached below.
4) At last the value of the coefficient of reflection is multiplied with Peak Incident Pressure to get the required Peak Reflected Pressure. The Peak Reflected Pressure is calculated for various Radial Distances at different Standoff Distances and TNT weights. The tubular results are attached herewith.

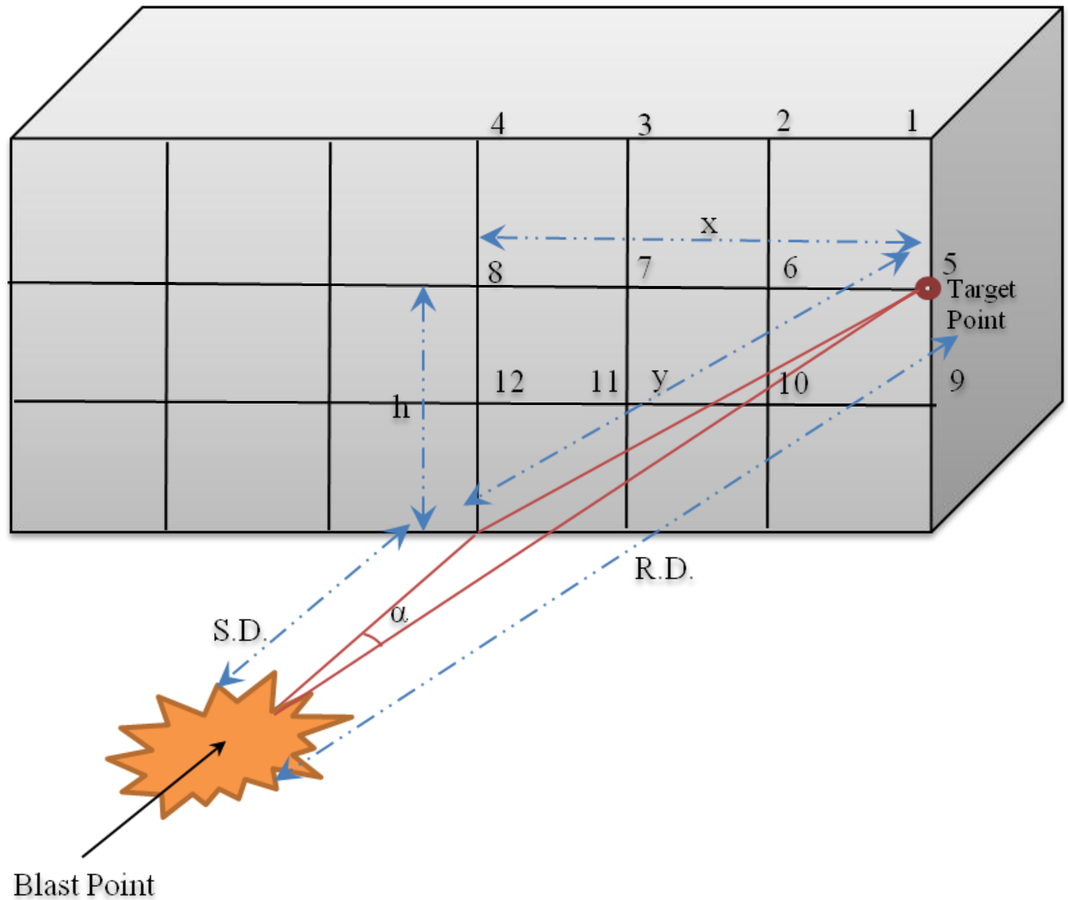

Fig. 4.2 Front face of Building showing various parameters

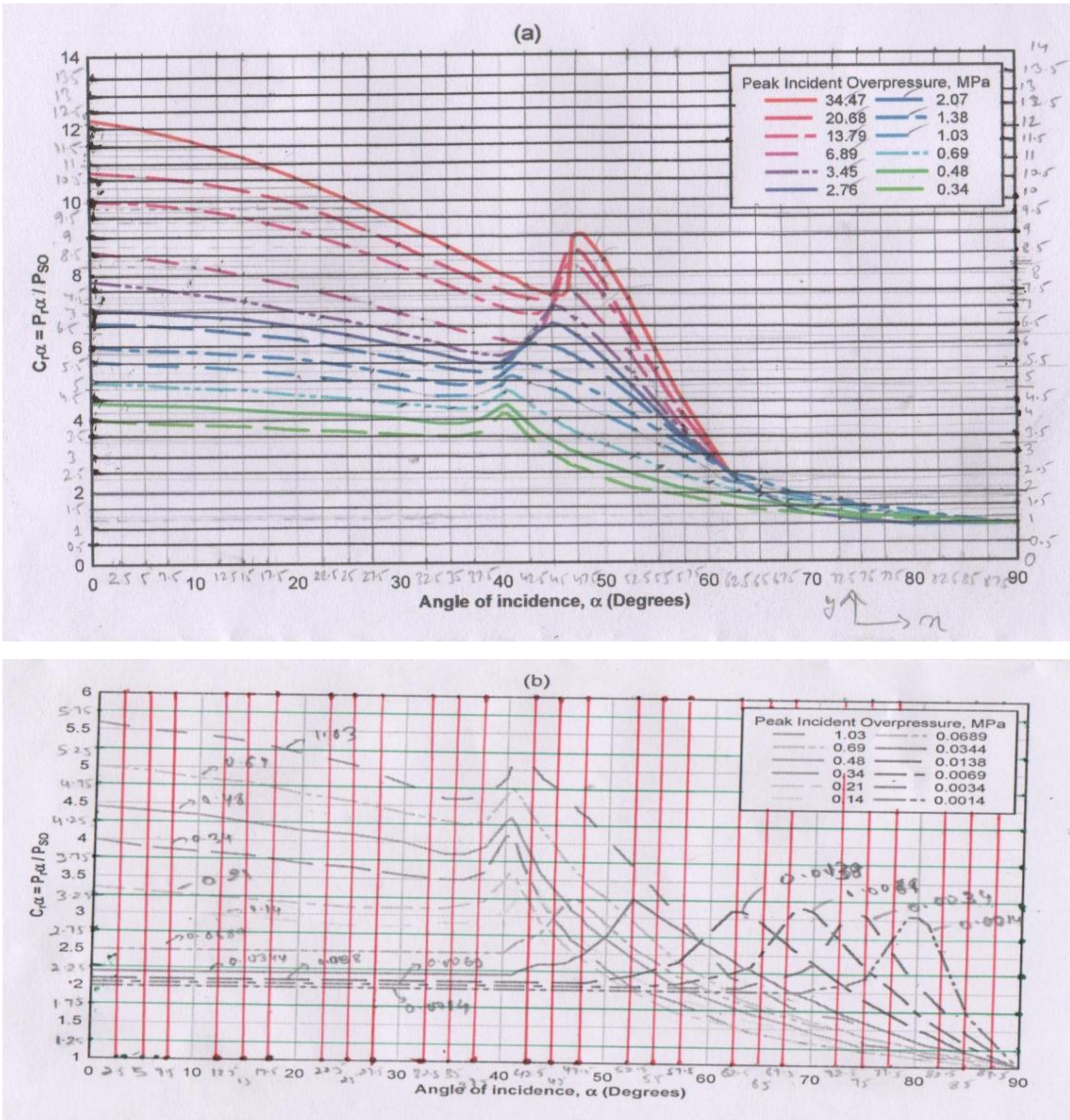

Figure 6: Influence of angle of incidence on the reflected pressure coefficient (a) for larger and (b) for smaller incident overpressure values (modified from [9]).

Fig. 4.3 UFC 3-340-02 (2008) Graphs discretized

a) From 34.7 MPa to 0.34 MPa

b) From 1.03 Mpa to 0.0014 MPa

Table 4.1 Calculation of Radial Distance and Angle of Incidence for different target points in front face of building for stand-off distance - 5m

S.No.	Coordinates of point in front of blast at base of the building			Co-ordinates of point vertically above & perpendicular to target point			Co-ordinates of target point			Standoff Distance	*h*	*x*	*y*	*R*	Alpha
	x_1	y_1	z_1	x_2	y_2	z_2	x'_2	y'_2	z'_2	S.D.(m)	(metre)	(metre)	(metre)	(metre)	(Degrees)
1	0.00	0.00	5.00	0.00	11.88	5.00	18.30	11.88	5.00	5.00	11.88	18.30	21.82	22.38	77.09
2	0.00	0.00	5.00	0.00	11.88	5.00	12.20	11.88	5.00	5.00	11.88	12.20	17.03	17.75	73.64
3	0.00	0.00	5.00	0.00	11.88	5.00	6.10	11.88	5.00	5.00	11.88	6.10	13.35	14.26	69.47
4	0.00	0.00	5.00	0.00	11.88	5.00	0.00	11.88	5.00	5.00	11.88	0.00	11.88	12.89	67.17
5	0.00	0.00	5.00	0.00	7.92	5.00	18.30	7.92	5.00	5.00	7.92	18.30	19.94	20.56	75.92
6	0.00	0.00	5.00	0.00	7.92	5.00	12.20	7.92	5.00	5.00	7.92	12.20	14.55	15.38	71.03
7	0.00	0.00	5.00	0.00	7.92	5.00	6.10	7.92	5.00	5.00	7.92	6.10	10.00	11.18	63.43
8	0.00	0.00	5.00	0.00	7.92	5.00	0.00	7.92	5.00	5.00	7.92	0.00	7.92	9.37	57.73
9	0.00	0.00	5.00	0.00	3.96	5.00	18.30	3.96	5.00	5.00	3.96	18.30	18.72	19.38	75.05
10	0.00	0.00	5.00	0.00	3.96	5.00	12.20	3.96	5.00	5.00	3.96	12.20	12.83	13.77	68.70
11	0.00	0.00	5.00	0.00	3.96	5.00	6.10	3.96	5.00	5.00	3.96	6.10	7.27	8.83	55.49
12	0.00	0.00	5.00	0.00	3.96	5.00	0.00	3.96	5.00	5.00	3.96	0.00	3.96	6.38	38.38

Table 4.2 Calculation of Radial Distance and Angle of Incidence for different target points in front face of the building for standoff distance-10m

S.No.	Co-ordinates of point in front of blast at base of the building			Co-ordinates of point vertically above & perpedicular to target point			Co-ordinates of target point			Standoff Distance	*h*	*x*	*y*	*R*	Alpha
	x_1	y_1	z_1	x_2	y_2	z_2	x'_2	y'_2	z'_2	S.D.	(metre)	(metre)	(metre)	(metre)	(Degrees)
1	0.00	0.00	10.00	0.00	11.88	10.00	18.30	11.88	10.00	10.00	11.88	18.30	21.82	24.00	65.37
2	0.00	0.00	10.00	0.00	11.88	10.00	12.20	11.88	10.00	10.00	11.88	12.20	17.03	19.75	59.58
3	0.00	0.00	10.00	0.00	11.88	10.00	6.10	11.88	10.00	10.00	11.88	6.10	13.35	16.68	53.17
4	0.00	0.00	10.00	0.00	11.88	10.00	0.00	11.88	10.00	10.00	11.88	0.00	11.88	15.53	49.91
5	0.00	0.00	10.00	0.00	7.92	10.00	18.30	7.92	10.00	10.00	7.92	18.30	19.94	22.31	63.37
6	0.00	0.00	10.00	0.00	7.92	10.00	12.20	7.92	10.00	10.00	7.92	12.20	14.55	17.65	55.49
7	0.00	0.00	10.00	0.00	7.92	10.00	6.10	7.92	10.00	10.00	7.92	6.10	10.00	14.14	44.99
8	0.00	0.00	10.00	0.00	7.92	10.00	0.00	7.92	10.00	10.00	7.92	0.00	7.92	12.76	38.38
9	0.00	0.00	10.00	0.00	3.96	10.00	18.30	3.96	10.00	10.00	3.96	18.30	18.72	21.23	61.89
10	0.00	0.00	10.00	0.00	3.96	10.00	12.20	3.96	10.00	10.00	3.96	12.20	12.83	16.26	52.06
11	0.00	0.00	10.00	0.00	3.96	10.00	6.10	3.96	10.00	10.00	3.96	6.10	7.27	12.36	36.03
12	0.00	0.00	10.00	0.00	3.96	10.00	0.00	3.96	10.00	10.00	3.96	0.00	3.96	10.76	21.60

Table 4.3 Peak Reflected Pressure for 50kg TNT Weight & 5m Stand-off Distance

Joint Number (Gauge point)	11	12	13	14	10	21	20	19	9	8	7	6
Radial distance (R) (metre)	22.38	17.75	14.26	12.89	20.56	15.38	11.18	9.37	19.38	13.77	8.83	6.38
Charge Weight (W) (kg)	50.00	50.00	50.00	50.00	50.00	50.00	50.00	50.00	50.00	50.00	50.00	50.00
Scaled Distance (Z) (kg/ m^3)	6.08	4.82	3.88	3.50	5.59	4.18	3.04	2.55	5.27	3.74	2.40	1.73
Peak Incident Pressure (kN/m^2)	20.52	30.82	47.17	58.15	23.69	40.54	79.01	117.38	26.27	50.67	134.47	286.25
Positive Time Duration (ms)	10.83	9.25	7.82	7.19	10.25	8.30	6.37	5.44	9.85	7.60	5.15	3.75
Posittive Impulse*(Ipos)*	0.32	0.40	0.50	0.55	0.35	0.46	0.62	0.72	0.37	0.51	0.76	0.95
Wave Decay Parameter (b)	18.69	9.62	4.88	3.51	14.75	6.21	2.19	1.26	12.46	4.36	1.08	0.79
Angle of incidence (Degree)	77.09	73.64	69.47	67.17	75.92	71.03	63.43	57.73	75.05	68.7	55.49	38.38
Cofficient of Refraction,($c_{r)}$	1.69	1.77	1.80	1.81	1.73	1.79	1.71	1.84	1.76	1.81	1.72	4.34
Peak Reflected Pressure (Pref) (kN/m^2)	34.58	54.69	84.79	105.38	40.99	72.42	135.18	216.34	46.17	91.63	231.94	1243.15

Table 4.4 Peak Reflected Pressure for 100kg TNT Weight & 5m Stand-off Distance

Joint Number (Gauge point)	11	12	13	14	10	21	20	19	9	8	7	6
Radial distance (R) (metre)	22.38	17.75	14.26	12.89	20.56	15.38	11.18	9.37	19.38	13.77	8.83	6.38
Charge Weight (W) (kg)	100.00	100.00	100.00	100.00	100.00	100.00	100.00	100.00	100.00	100.00	100.00	100.00
Scaled Distance (Z) (kg/ m^3)	4.83	3.83	3.08	2.78	4.44	3.32	2.41	2.02	4.18	2.97	1.91	1.38
Peak Incident Pressure (kN/m^2)	30.76	48.33	76.87	96.17	36.11	65.25	132.89	200.09	40.51	83.02	229.80	488.12
Positive Time Duration (ms)	11.46	9.64	8.04	7.37	10.78	8.58	6.49	5.50	10.32	7.81	5.20	3.69
Posittive Impulse*(Ipos)*	0.40	0.50	0.61	0.67	0.44	0.57	0.75	0.86	0.46	0.63	0.89	1.06
Wave Decay Parameter (b)	9.65	4.70	2.28	1.64	7.47	2.93	1.09	0.81	6.21	2.03	0.78	1.00
Angle of incidence (Degree)	77.09	73.64	69.47	67.17	75.92	71.03	63.43	57.73	75.05	68.7	55.49	38.38
Cofficient of Refraction,($c_{r)}$	1.56	1.63	1.46	1.50	1.58	1.57	1.60	1.21	1.62	1.47	2.10	4.98
Peak Reflected Pressure (Pref) (kN/m^2)	48.01	78.67	112.02	144.16	57.20	102.22	212.60	242.11	65.52	122.33	482.81	2429.84

Table 4.5 Peak Reflected Pressure for 50kg TNT Weight & 10m Stand-off Distance

Joint Number (Gauge point)	11	12	13	14	10	21	20	19	9	8	7	6
Radial distance (R) (metre)	24.00	19.75	16.68	15.53	22.31	17.65	14.14	12.76	21.23	16.26	12.36	10.76
Charge Weight (W) (kg)	50.00	50.00	50.00	50.00	50.00	50.00	50.00	50.00	50.00	50.00	50.00	50.00
Scaled Distance (Z) (kg/ m^3)	6.52	5.37	4.53	4.22	6.06	4.80	3.84	3.47	5.77	4.42	3.36	2.92
Peak Incident Pressure (kN/m^2)	18.31	25.41	34.62	39.78	20.63	31.14	47.99	59.44	22.42	36.35	63.51	86.06
Positive Time Duration(ms)	11.31	9.98	8.84	8.36	10.81	9.21	7.76	7.13	10.47	8.67	6.95	6.16
Posittive Impulse*(Ipos)*	0.30	0.36	0.43	0.46	0.32	0.40	0.50	0.55	0.34	0.44	0.57	0.64
Wave Decay Parameter (b)	22.62	13.15	7.98	6.40	18.53	9.47	4.75	3.39	16.14	7.39	3.06	1.93
Angle of incidence (Degree)	65.37	59.58	53.17	49.91	63.37	55.49	44.99	38.38	61.89	52.06	36.03	21.60
Cofficient of Refraction,(c_{r})	2.78	2.71	3.00	2.85	2.74	2.97	2.63	2.48	2.70	2.93	2.52	2.96
Peak Reflected Pressure (Pref) (kN/m^2)	50.90	68.76	103.70	113.18	56.48	92.49	126.05	147.60	60.63	106.45	160.12	254.60

Table 4.6 Peak Reflected Pressure for 100kg TNT Weight & 10m Stand-off Distance

Joint Number (Gauge point)	11	12	13	14	10	21	20	19	9	8	7	6
Radial distance (R) (metre)	24.00	19.75	16.68	15.53	22.31	17.65	14.14	12.76	21.23	16.26	12.36	10.76
Charge Weight (W) (kg)	100.00	100.00	100.00	100.00	100.00	100.00	100.00	100.00	100.00	100.00	100.00	100.00
Scaled Distance (Z) (kg/ m^3)	5.18	4.26	3.60	3.35	4.81	3.81	3.05	2.75	4.58	3.51	2.67	2.32
Peak Incident Pressure (kN/m^2)	27.08	39.04	54.93	63.92	30.95	48.88	78.31	98.44	33.97	57.94	105.61	145.28
Positive Time Duration (ms)	12.03	10.46	9.17	8.64	11.44	9.59	7.99	7.30	11.04	8.98	7.10	6.26
Posittive Impulse*(Ipos)*	0.38	0.45	0.53	0.57	0.40	0.50	0.62	0.68	0.42	0.54	0.69	0.78
Wave Decay Parameter (b)	11.86	6.59	3.84	3.03	9.56	4.61	2.22	1.59	8.23	3.53	1.45	1.00
Angle of incidence (Degree)	65.37	59.58	53.17	49.91	63.37	55.49	44.99	38.38	61.89	52.06	36.03	21.60
Cofficient of Refraction,(c_r)	2.48	2.56	2.74	2.91	2.46	2.74	3.06	3.21	2.48	2.77	3.16	3.48
Peak Reflected Pressure (Pref)(kN/m^2)	67.07	99.96	150.47	185.93	76.06	133.95	239.86	316.12	84.12	160.46	333.74	505.23

4.3 Calculation of Blast Pressure in ANSYS

4.3.1 Modeling of building in ANSYS

Modeling of the building is done in ANSYS workbench Static Structural. In static structural, the various steps followed are shown below. After applying loads to building it can be analyzed for finding different parameters like displacement, bending moments, stresses etc.

Generation of points according to the geometry of the building

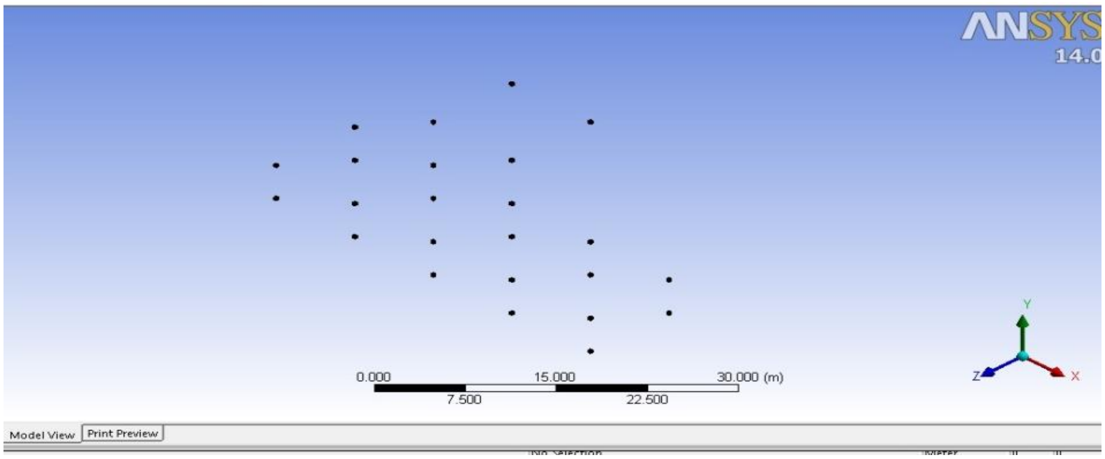

Fig. 4.4 Generation of points

Joining of points to make the given building as per dimensions.

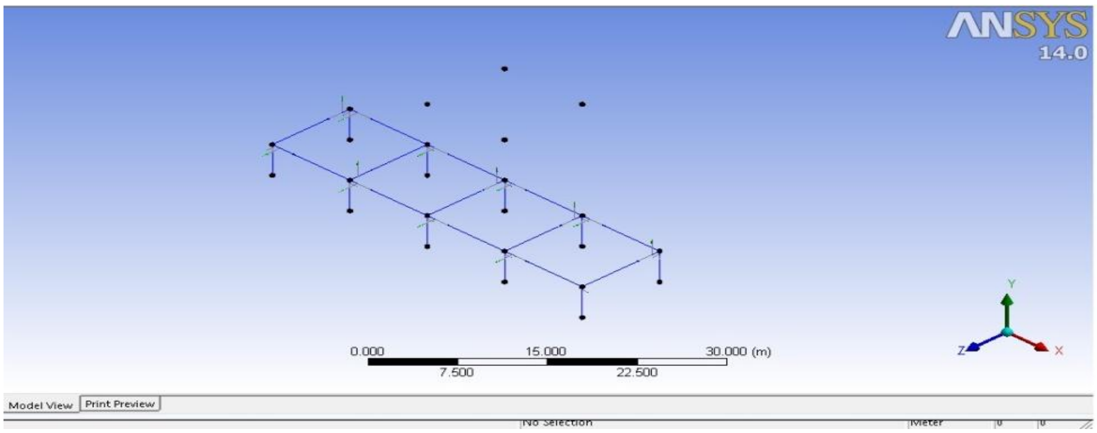

Fig. 4.5 Joining of points with lines

Specifying cross-section for beams and columns and generation of slab of appropriate thickness

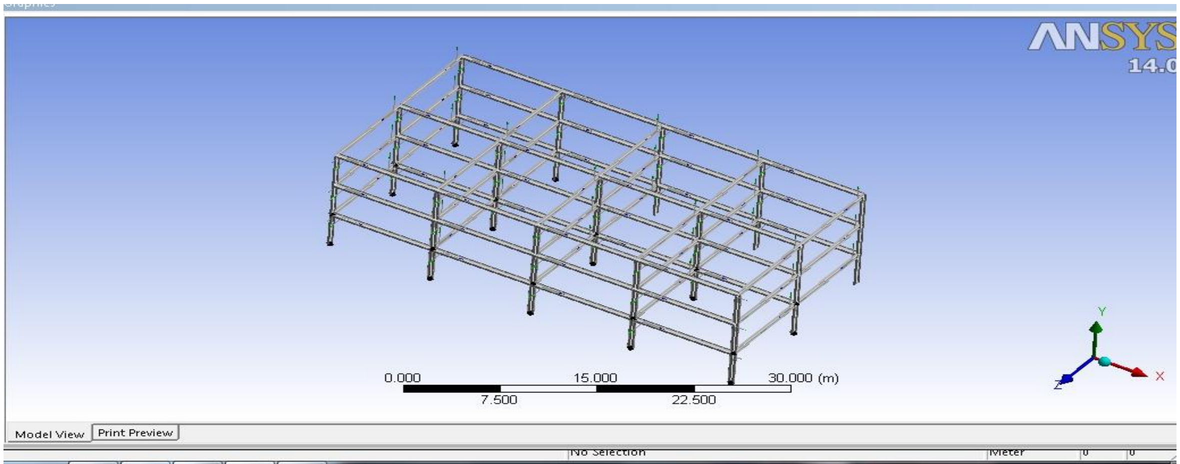

Fig. 4.6 Cross-section allotment to beams and columns

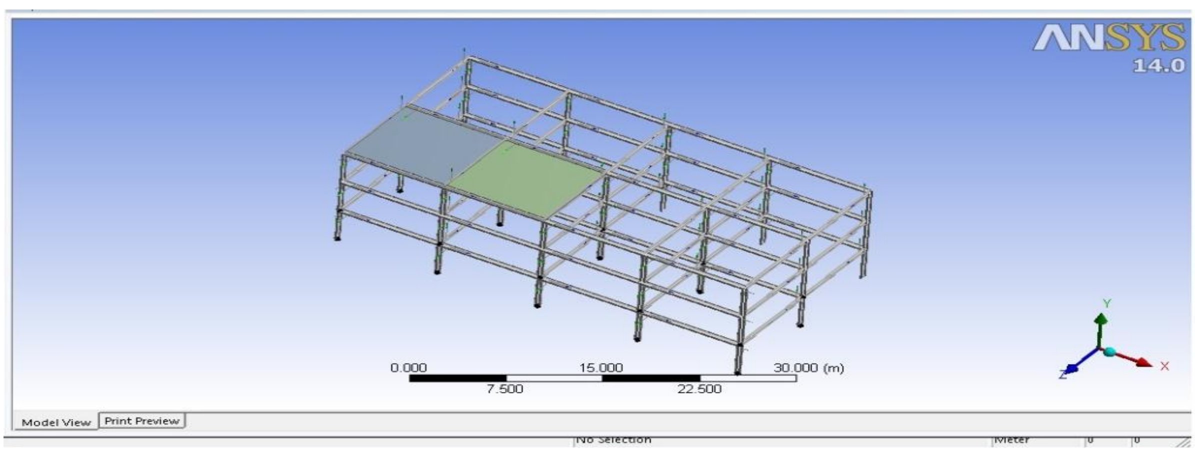

Fig. 4.7 Slab generation

Meshing and Application of Loads

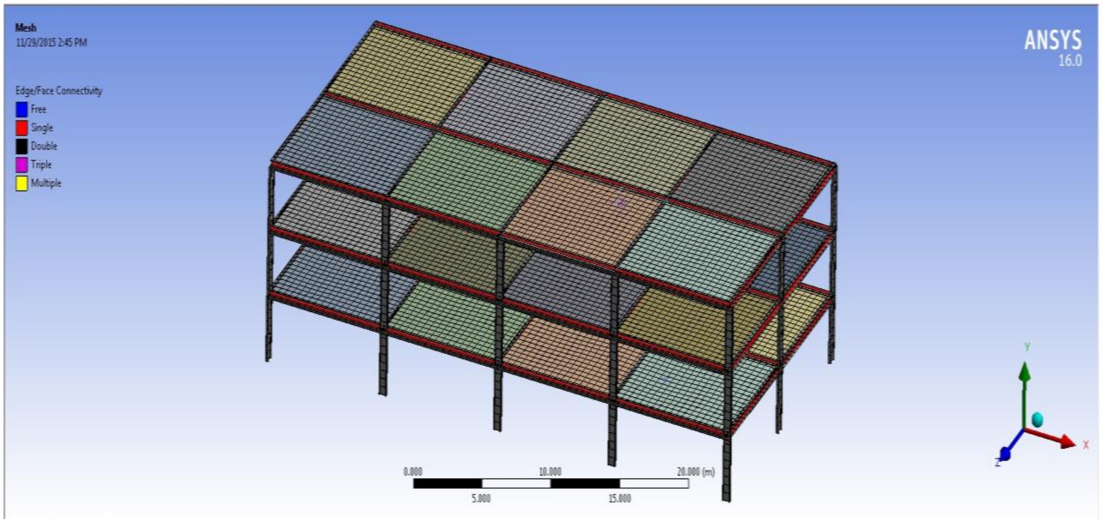

Fig 4.8 Meshing of building

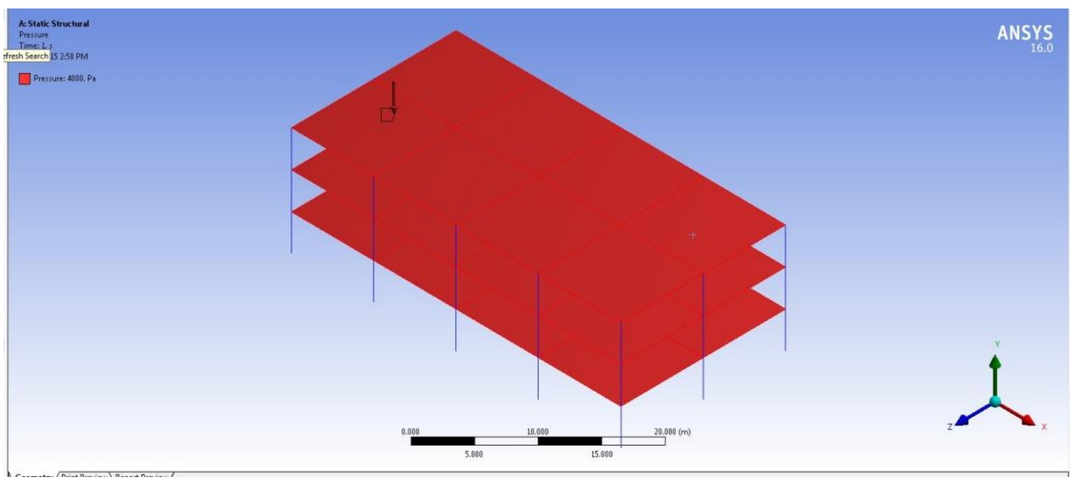

Fig. 4.9 Application of loads

4.4 AUTODYN analysis of Building subjected to Blast Loading

4.4.1 Introduction to Autodyn

ANSYS Autodyn software is a versatile explicit analysis tool for modeling the nonlinear dynamics of solids, fluids, gases and their interactions. The product has been developed to provide advanced capabilities within a robust, easy-to-use software tool. Simulation projects can be completed with significantly less effort, less time and lower labor costs than with other explicit programs. This high productivity is a result of the quick-to-learn, intuitive, interactive graphical interface implemented. Time and effort are saved in problem setup and analysis by automatic options to define contact, by coupling interfaces and by minimizing input requirements using safe logical defaults.

4.4.2 Equation of State

An equation of state describes the hydrodynamic response of a material. This is the primary response for gases and liquids, which can sustain no shear. Their response to dynamic loading is assumed hydrodynamic, with pressure varying as a function of density and internal energy. This is also the primary response for solids at high deformation.

4.4.3 JWL equation of state

The JWL equation of state describes the detonation product expansion down to a pressure of 1 kilo bar for high energy explosive materials. It has been proposed by Jones, Wilkins and Lee according to following equation

$$p = A\left(1-\frac{w\eta}{R_1}\right)e^{\frac{-R_1}{\eta}} + B\left(1-\frac{w\eta}{R_2}\right)e^{\frac{-R_1}{\eta}} + w\rho e \quad (4.1)$$

where ρ_0 is reference density, ρ density and $\eta = \rho/\rho_0$

The values of the constants *A, B, R1,* R_2 *and* ω for many common explosives have been determined from dynamic experiments.

The standard JWL equation of state can be used in combination with an energy release extension whereby additional energy is deposited over a user-defined time interval. Thermo baric explosives show this behavior and produce more explosive energy than conventional high energy explosives through combustion of inclusions, like aluminum, with atmospheric oxygen after detonation.

4.4.4. Procedure

The building modelled in ANSYS workbench Static Structural is then transferred to Explicit Dynamics which will help us to transfer to Autodyn where we can apply Blast Load on it. In Autodyn, the block of steel has been put in the air medium. Then blast is placed at the required point and its effect on building can be seen in the air contours. The procedure is explained below.

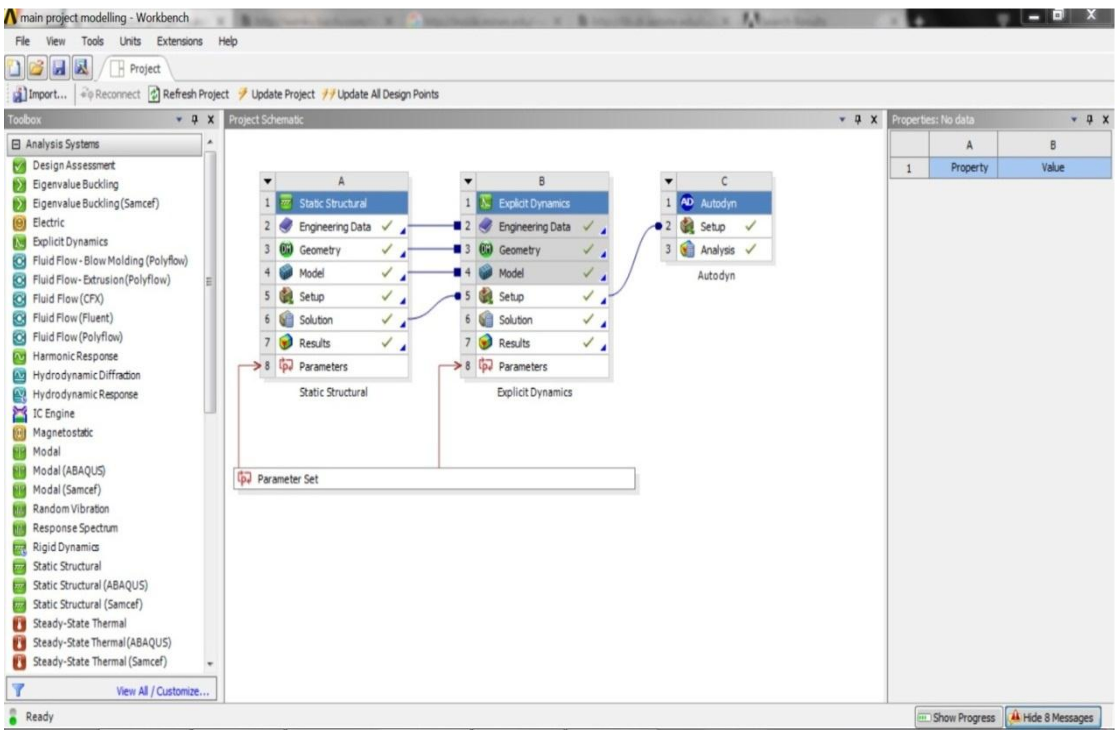

Fig. 4.10 Workbench Layout

Generating the steel block and providing air medium around it.

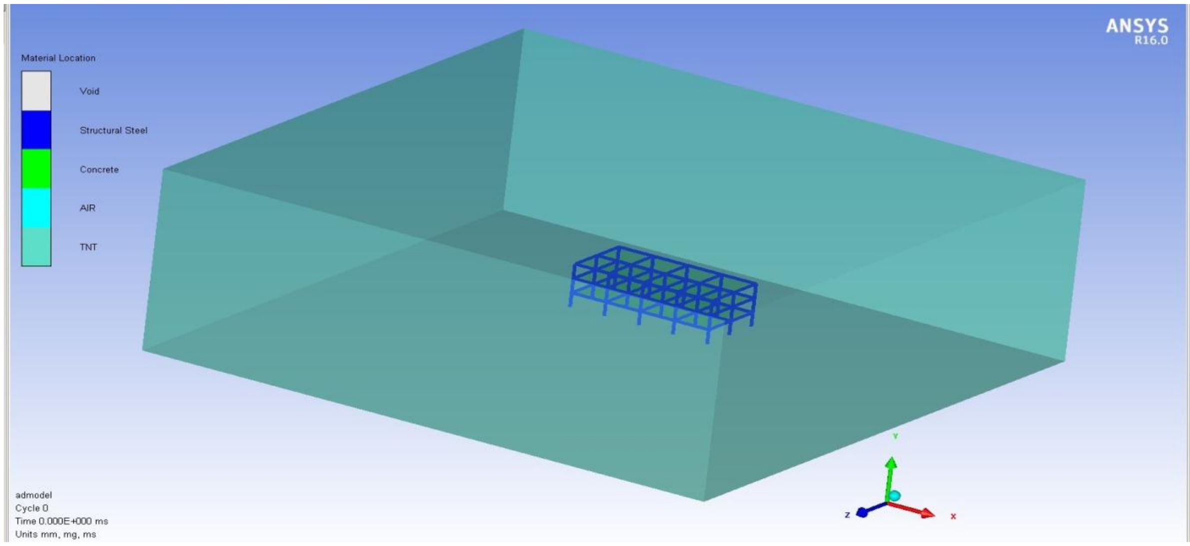

Fig. 4.11Air Medium surrounding Building

Gauge points

The Gauge points are the points where we can find the required parameters like pressure velocity after the explosion.

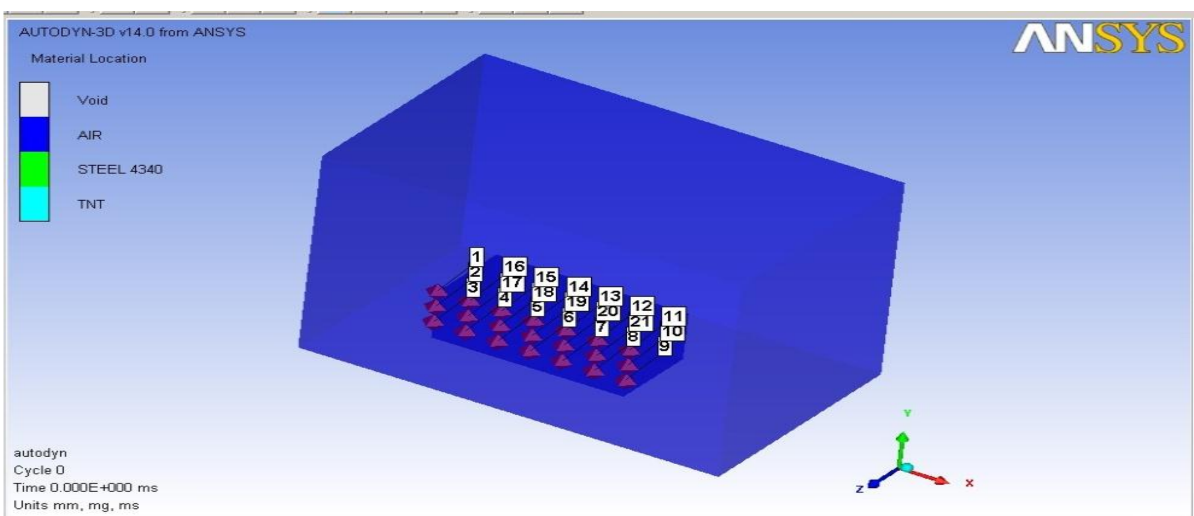

Fig. 4.12 Gauge Points

Placement of blast at required point.

The blast load is placed in the form of sphere of radius as per weight if TNT at the required point. The red dot in fig. below denotes its position.

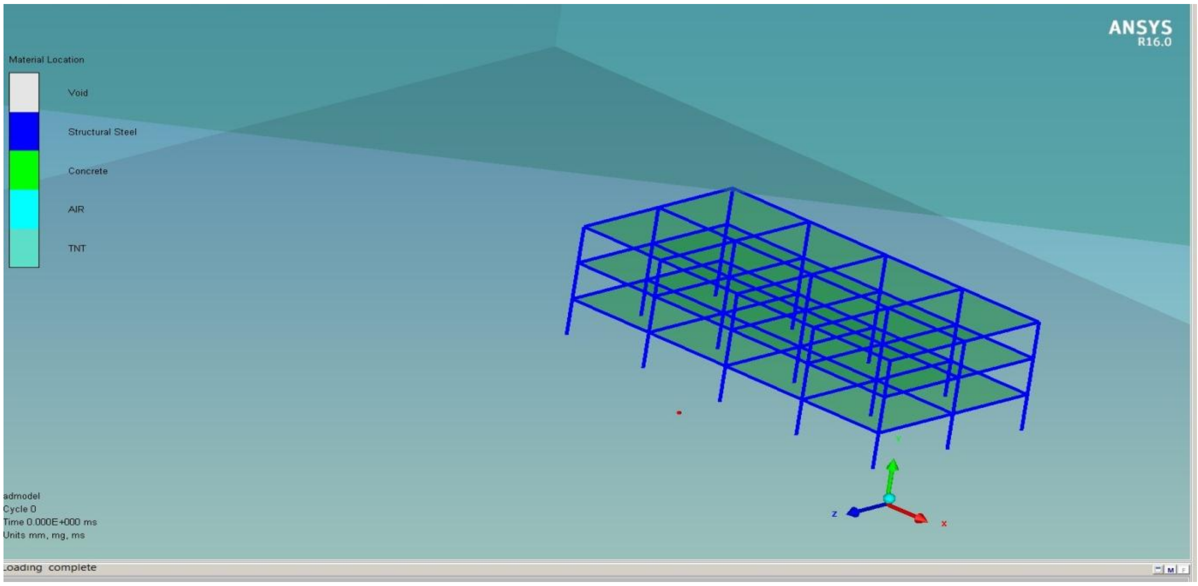

Fig. 4.13 Blast point in front of building

Blast waves after explosion

The blast waves can be seen after the explosion had taken place. The different colors show the different values of pressure of maximum to minimum intensities.

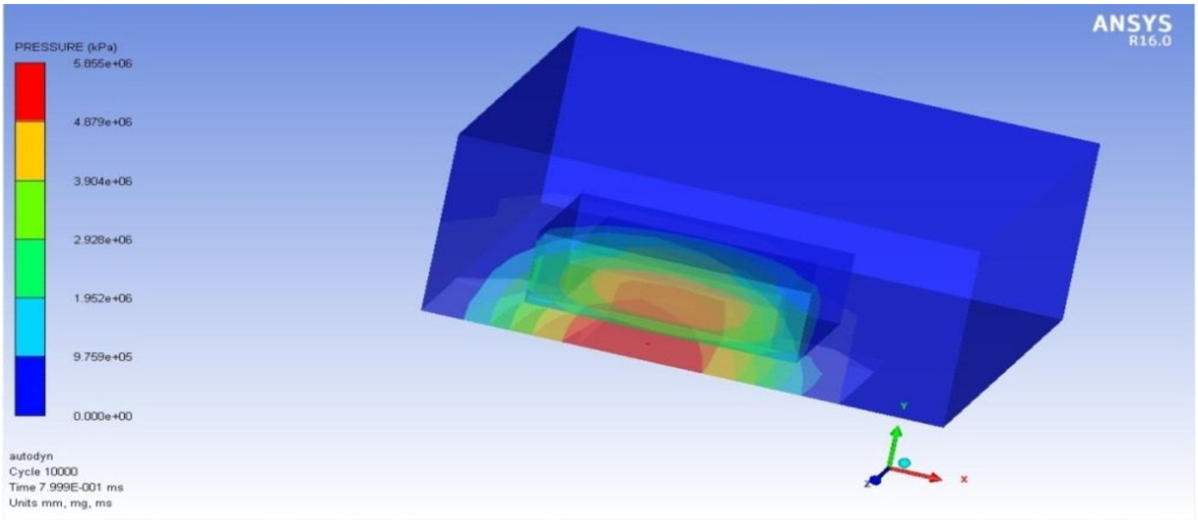

Fig. 4.14 Blast waves

4.5 Peak Reflected Pressure in Autodyn

Table 4.7 Peak Reflected Pressure on gauge Points in Building for 50 kg TNT

Joint Number	Peak Reflected Pressure at 5m Stand-off Distance (kN/m^2)	Peak Reflected Pressure at 10m Stand-off Distance (kN/m^2)
1.	29.74	43.77
2.	51.95	65.32
3.	78.86	96.44
4.	91.68	98.47
5.	35.25	48.57
6.	64.45	82.32
7.	113.55	105.88
8.	186.06	126.94
9.	38.78	50.93
10.	79.72	92.61
11.	208.75	144.11
12.	1143.7	234.23

Table 4.8 Peak Reflected Pressure on gauge Points in Building for 100kg TNT

Joint Number	Peak Reflected Pressure at 5m Stand-off Distance (kN/m^2)	Peak Reflected Pressure at 10m Stand-off Distance (kN/m^2)
1.	41.29	57.67
2.	74.73	94.96
3.	104.18	139.94
4.	125.42	161.76
5.	49.19	65.41
6.	90.97	119.22
7.	178.59	201.48
8.	208.22	271.87
9.	55.03	70.66
10.	106.43	139.60
11.	434.53	300.37
12.	2235.45	464.82

4.6 Observation made from both the Results

- Peak Reflected Pressure calculate**d by Kinney - Graham** approach is slightly more than that computed from Autodyn Analysis on building.
- The percentage of increase in Pressure is between 8% to 17% than that calculated by Autodyn analysis.
- Peak Reflected Pressure is more for 50kg 10m than 50kg 5m at some points in the upper storeys because the angle of incidence is less at those points which increases the coefficient of refraction values and hence peak Reflected Pressure.

CHAPTER 5

COMPARATIVE STUDY OF DIFFERENT COLUMN SECTIONS

5.1 General

Comparative study of 4 column sections has been carried out. The sections are of same cross sectional area and shapes are I-section, Rectangular box section, Channel section and Circular section. The sizes of column sections are

I-section: W14 × 99.

Rectangular box section: 50.8 × 30.5 × 1.27cm

Channel section: 65 × 13cm. Thickness of Flange: 2.5cm, Thickness of web: 2cm.

Circular section: 457 × 12.7mm

5.2 Results of Analysis

Following figures shows the process of explosion in Autodyn and also the deformed shapes of column due to blast.

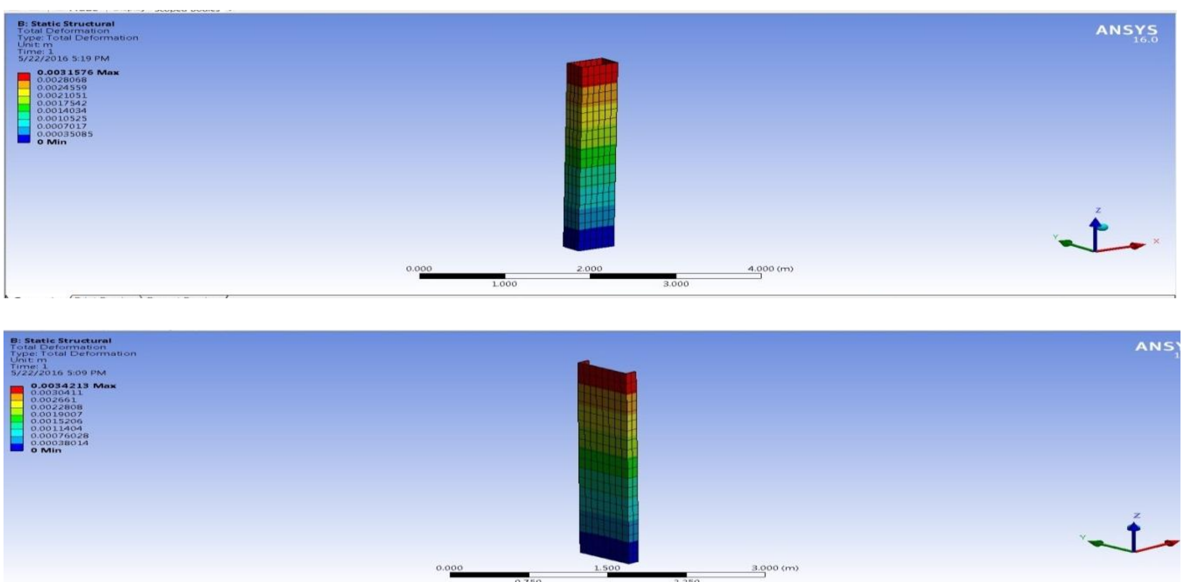

Fig. 5.1 Deformation in Rectangular box section and Channel section

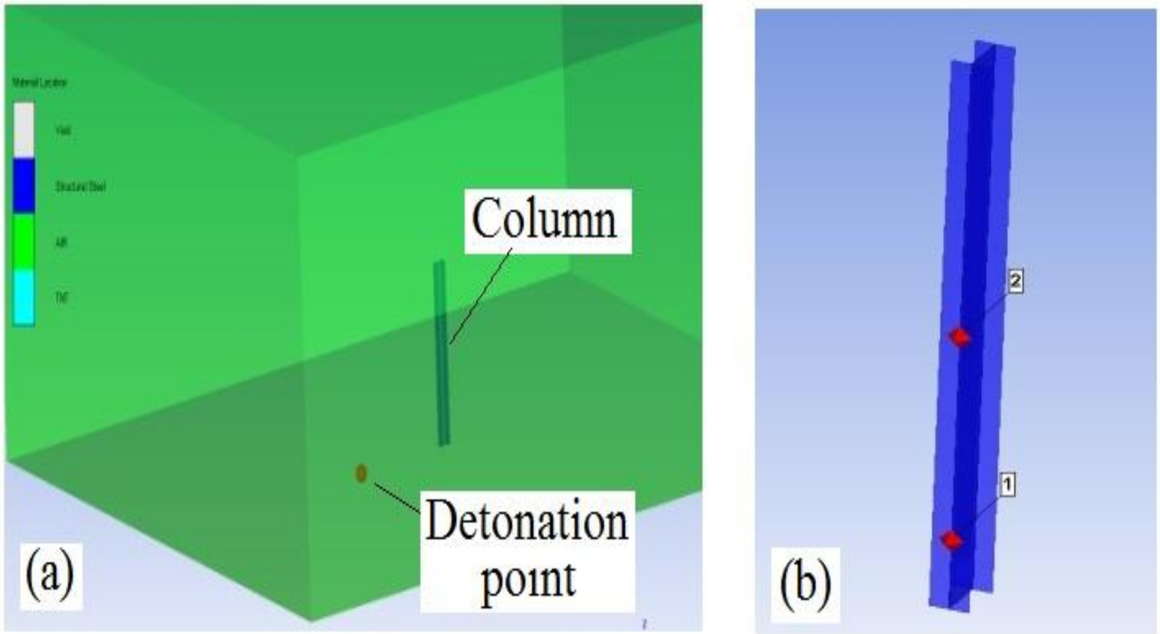

Fig. 5.2 (a) Column and detonation point, (b) Gauge points for response computation.

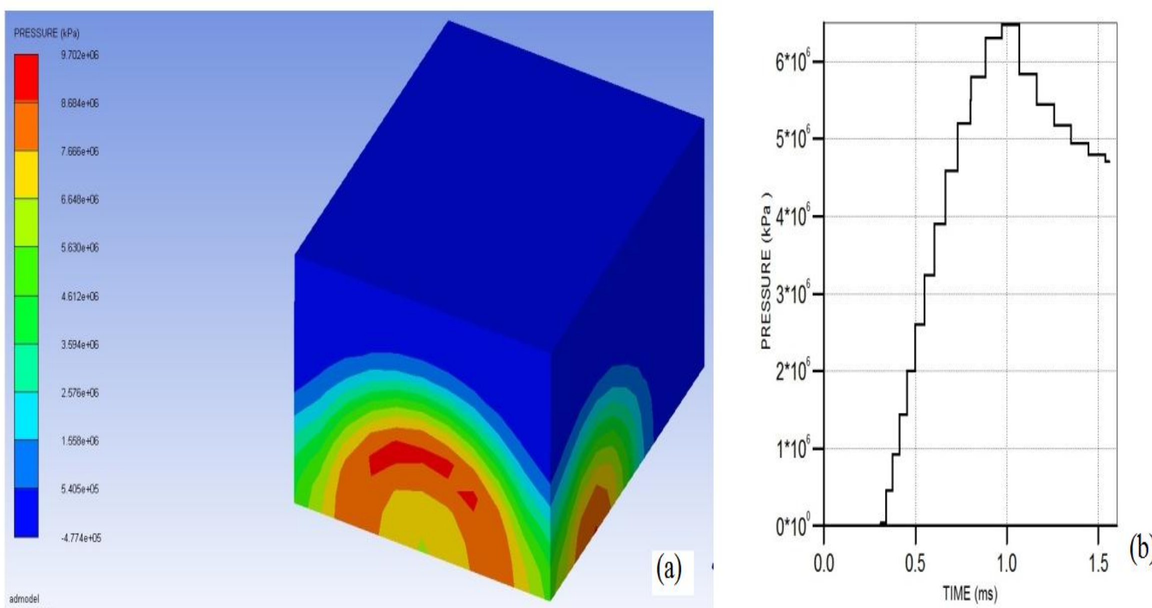

Fig. 5.3: (a) Pressure contours in air around column, (b) Peak pressure-time history on column.

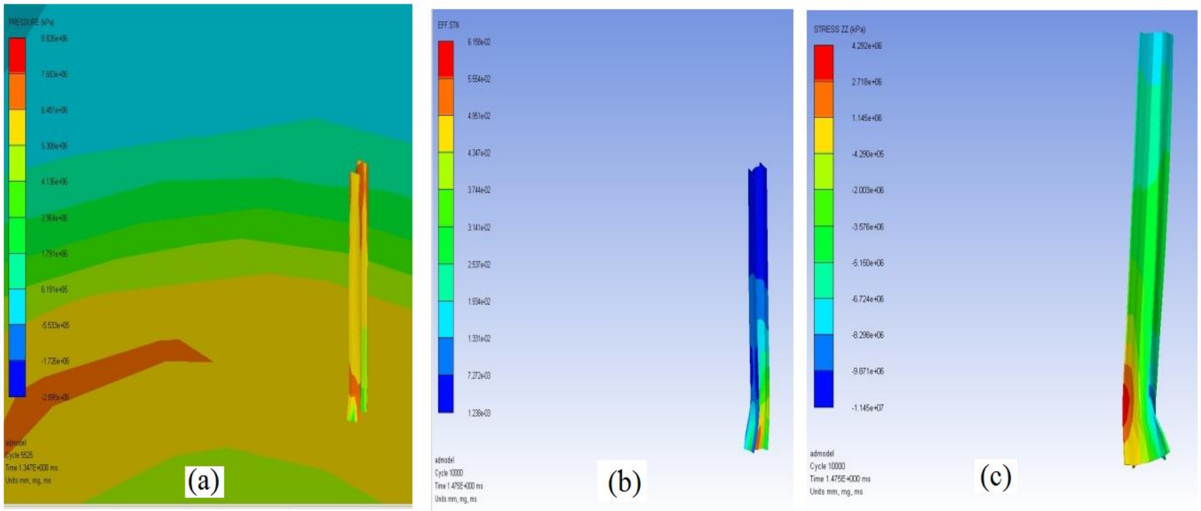

Fig. 5.4 (a) Blast pressure on column, (b) principal strain contours, and (c) Principal stress contours due to blast load at 1.47 ms.

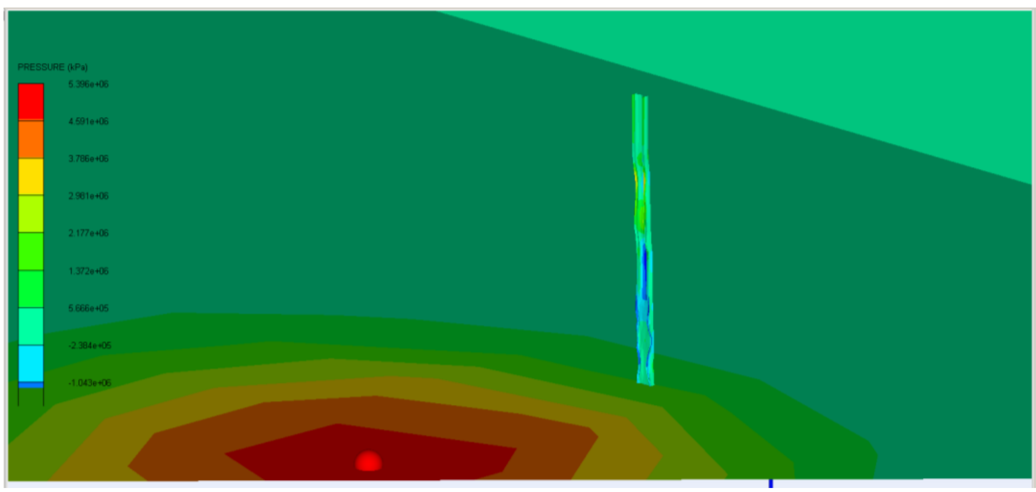

Fig. 5.5 Deformed column due to blast

5.3 Graphical Results

Graphical results are computed at gauge points for varied stand-off distances and Charge weights for different sections.

5.3.1 Variation of Pressure with Time at different TNT weights for different sections

<u>For I-section</u>

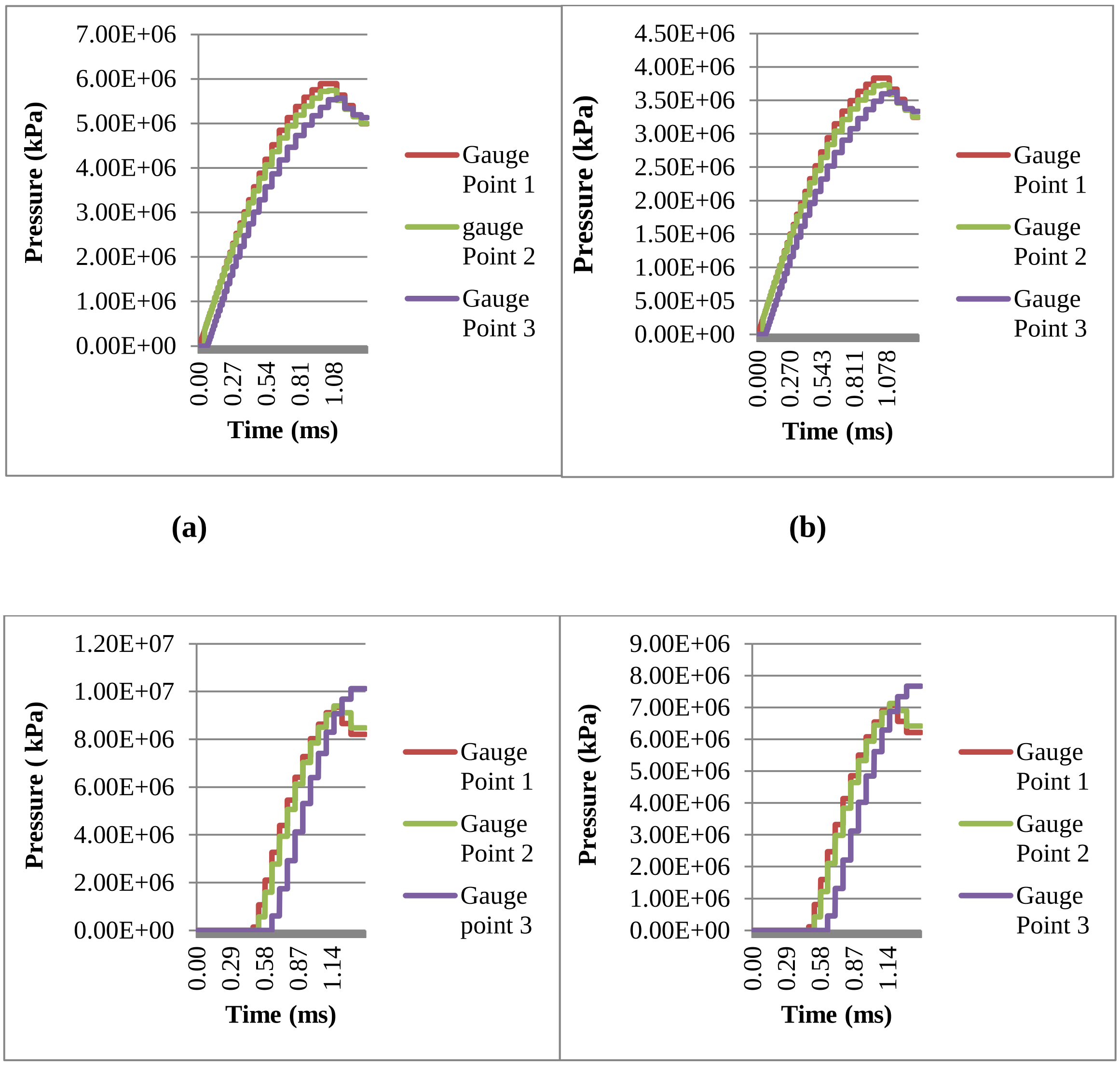

(c) **(d)**

Fig 5.6 Pressure vs Time for I-section (a) 50kg and 3m (b) 50kg and 5m (c)100kg and 3m (d) 100kg and 5m.

<u>Rectangular Box section</u>

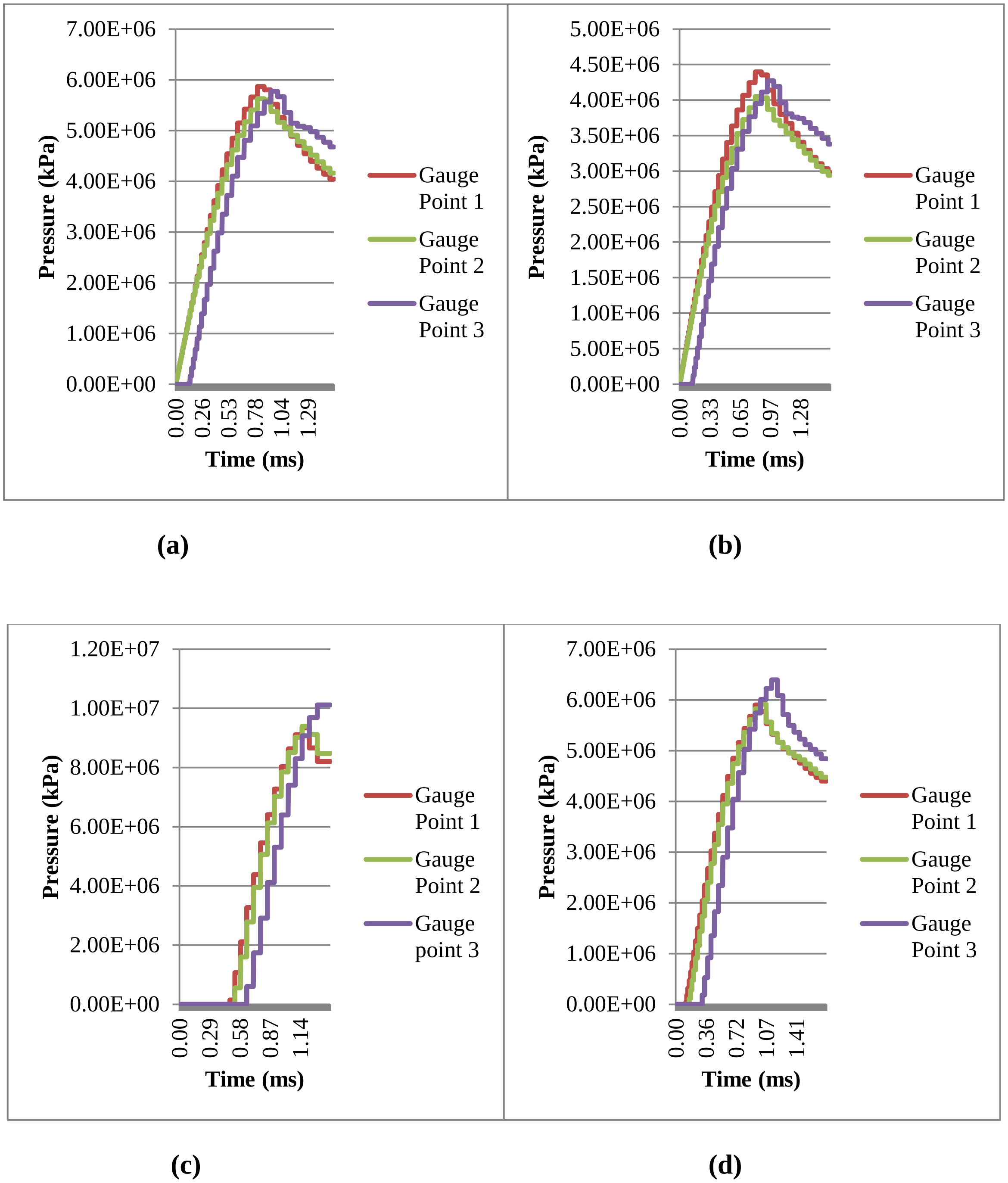

Fig 5.7 Pressure vs Time for R. B. section (a) 50kg and 3m (b) 50kg and 5m (c) 100kg and 3m (d) 100kg and 5m.

<u>**Channel section**</u>

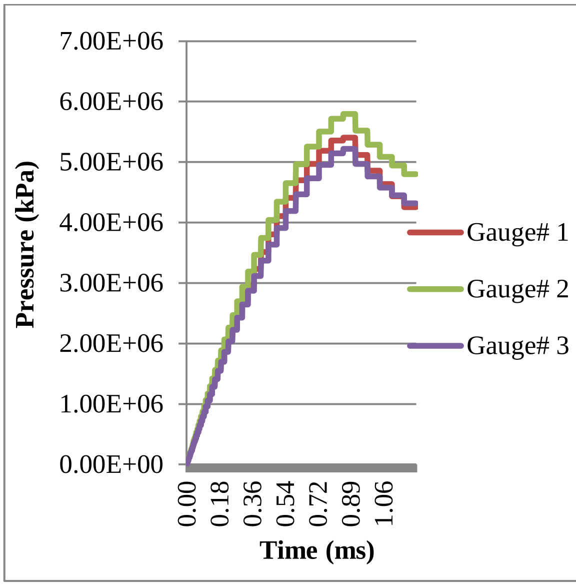

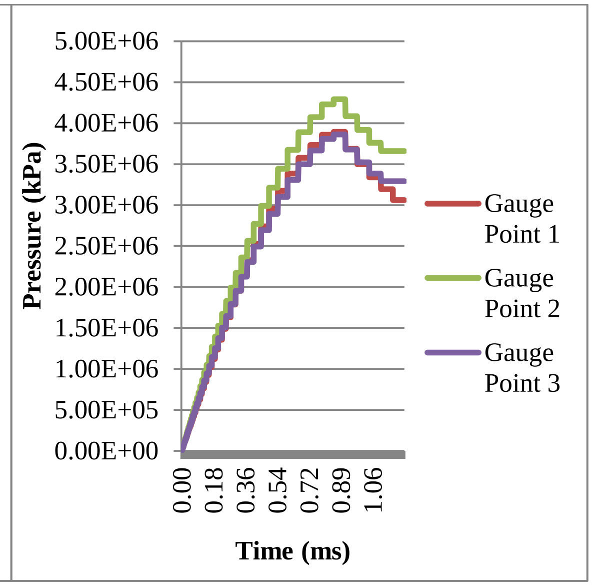

(a) **(b)**

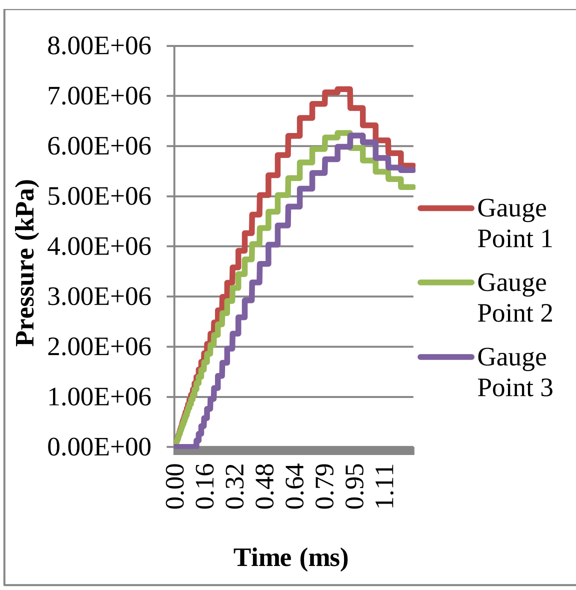

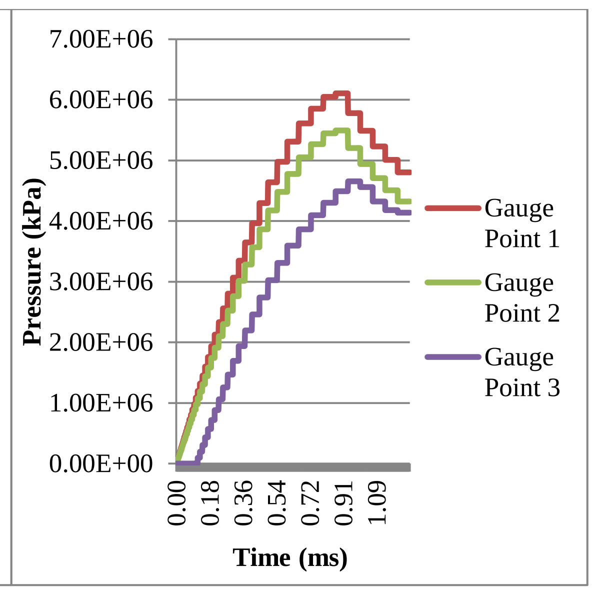

(c) **(d)**

Fig 5.8 Pressure vs Time for Channel section (a) 50kg and 3m (b) 50kg and 5m (c) 100kg and 3m (d) 100kg and 5m.

Circular Section

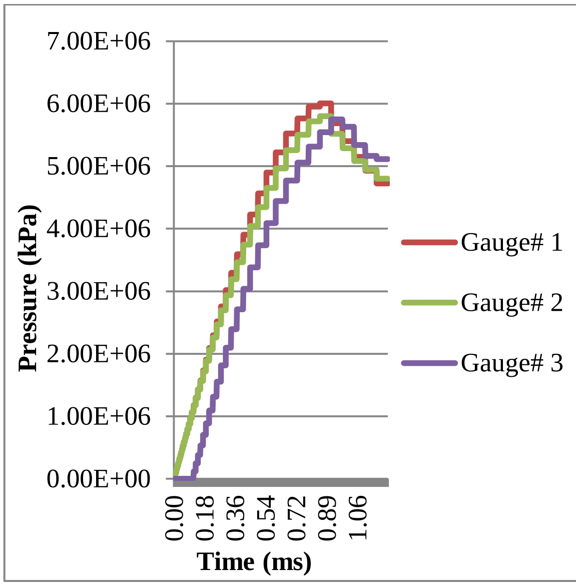

(a)

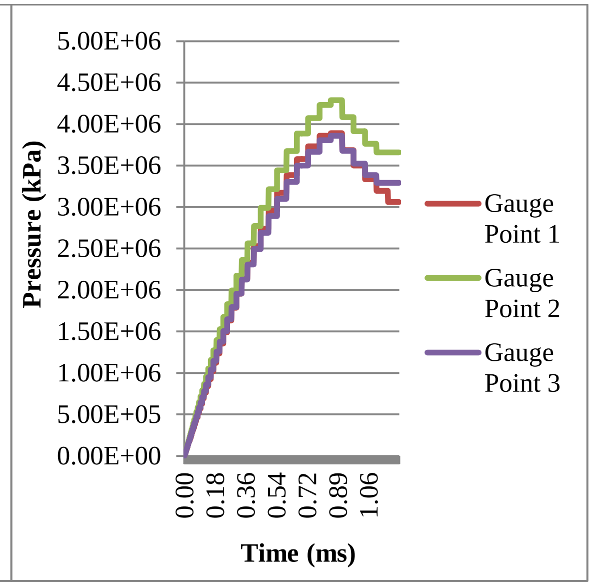

(b)

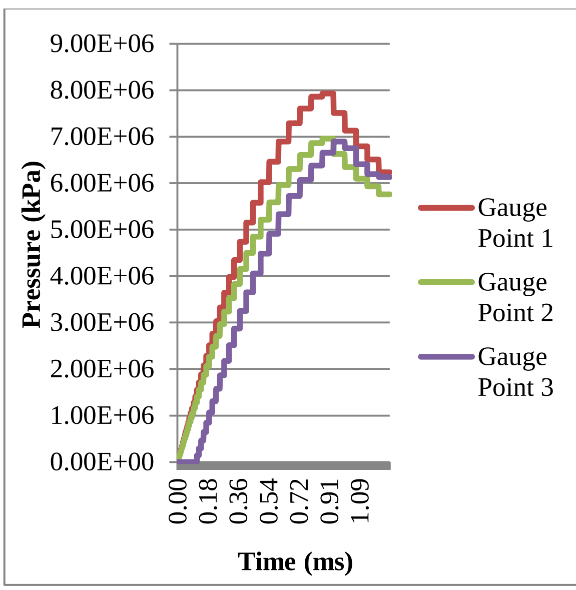

(c)

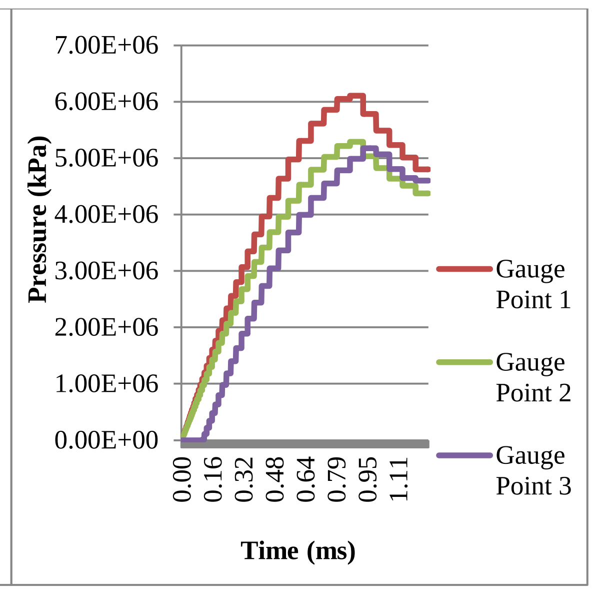

(d)

Fig 5.9 Pressure vs Time for Circular section (a) 50kg and 3m (b) 50kg and 5m (c) 100kg and 3m (d) 100kg and 5m.

5.3.2 Observations made from the above results

- Pressure is calculated for different stand-off distances and TNT weights at various gauge points.
- From the above graphs it is clear that the Pressure i.e. Peak Reflected Pressure will firstly take some fractions of milli-seconds to initiate and then increases abruptly within a few milli - seconds to a maximum value.
- After reaching maximum value, Pressure starts decreasing.
- Pressure will be maximum at first gauge point as it is near most to the blast point.
- For small stand-off distances like 3m, the pressure at gauge points 1& 2 will increase with same rate.

5.3.3 Kinetic Energy for different Standoff Distances and TNT weights for different sections

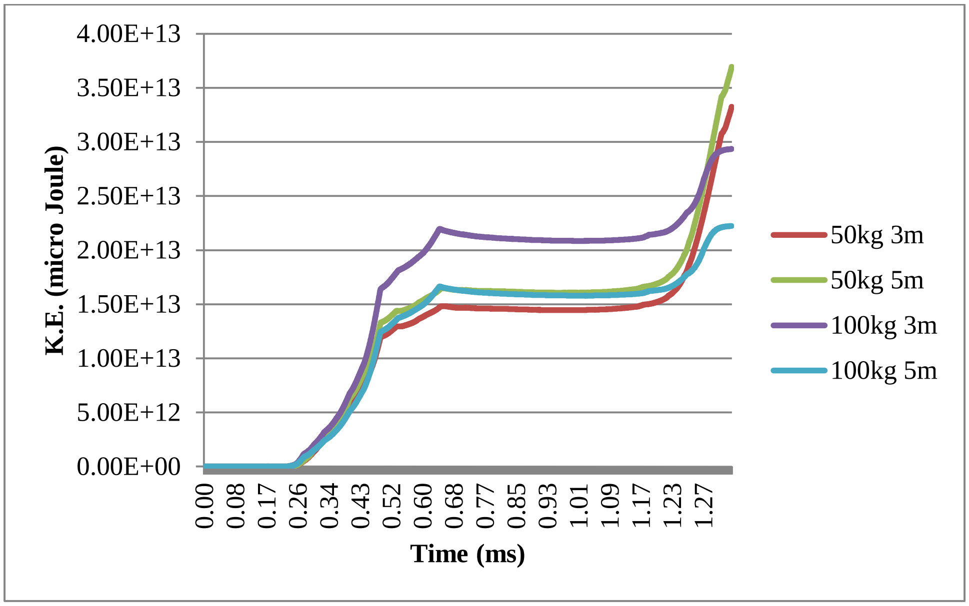

Fig. 5.10 Kinetic Energy for different charge weights and Stand-off distances for I-section

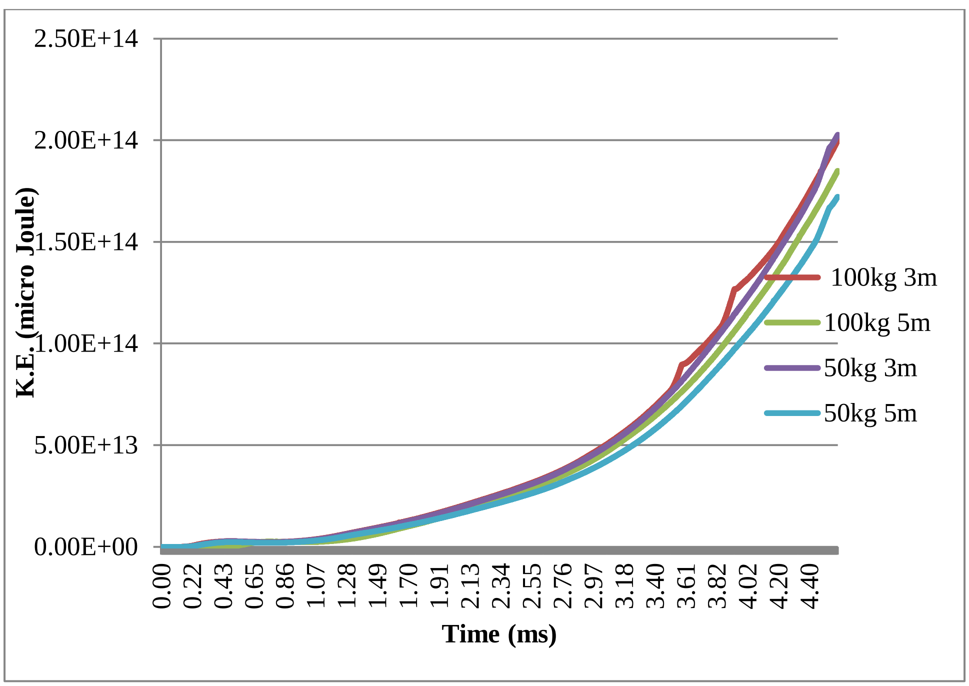

Fig 5.11 Kinetic Energy for different TNT weights and Stand-off distances for Rectangular Box section

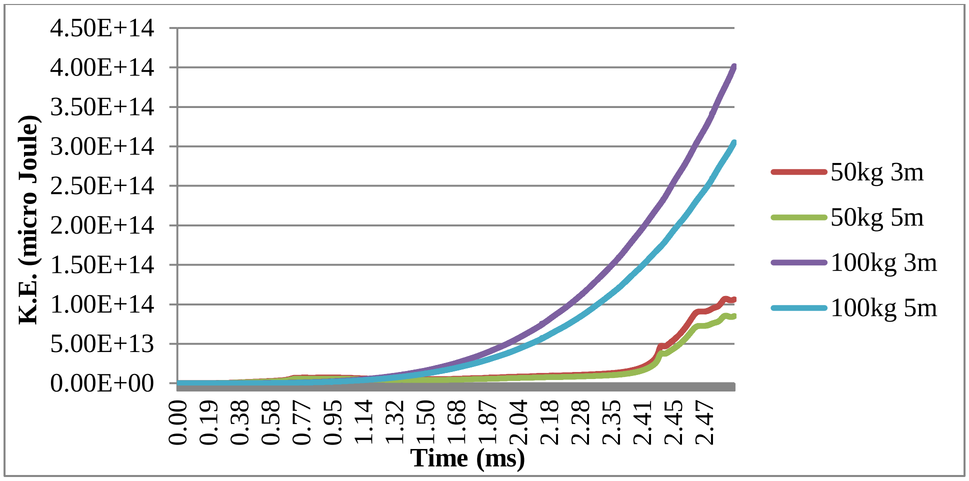

Fig 5.12 Kinetic Energy for different TNT weights and Stand-off distances for Circular section

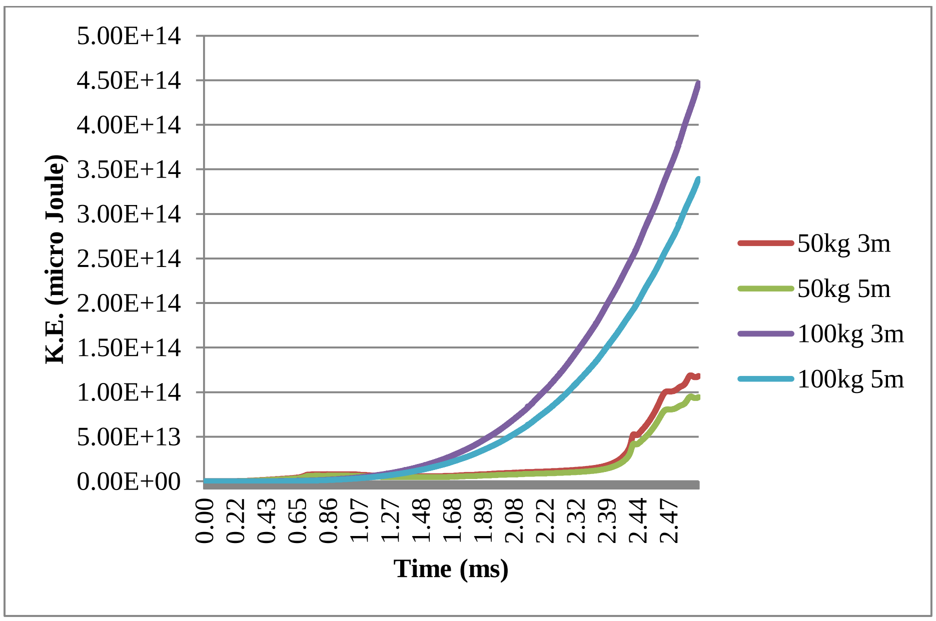

Fig 5.13 Kinetic Energy for different TNT weights and Stand-off distances for channel section

5.3.4 Conclusions drawn from above observations

- From the above graphs, it is observed that the K.E. is maximum for small stand-off distance and large TNT weights and vice-versa.
- K.E. first increases and then decreases suddenly to zero value when material fails.

5.3.5 Variation of Different Parameters for different TNT weights and Stand-off Distances for I-section

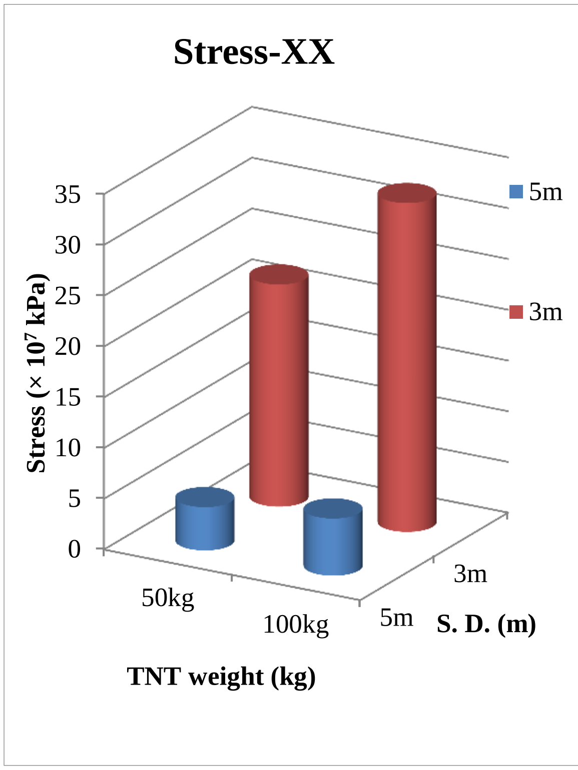

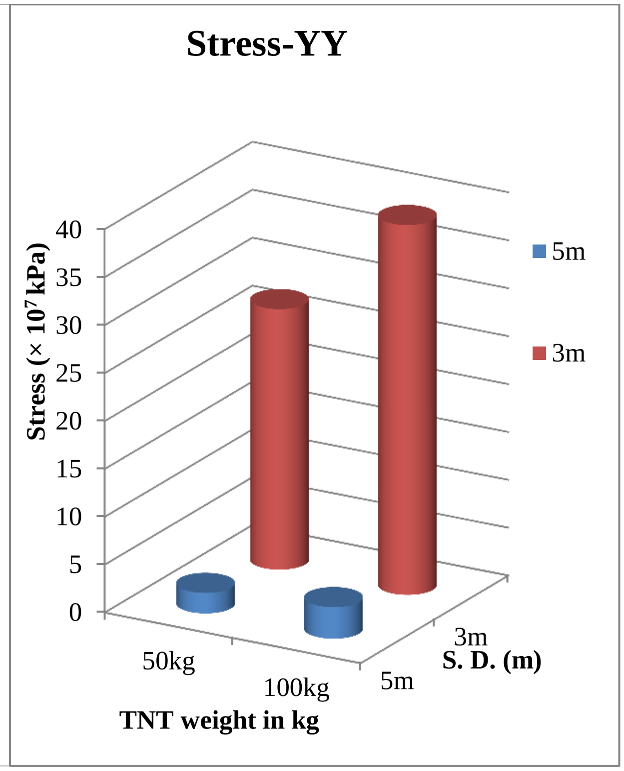

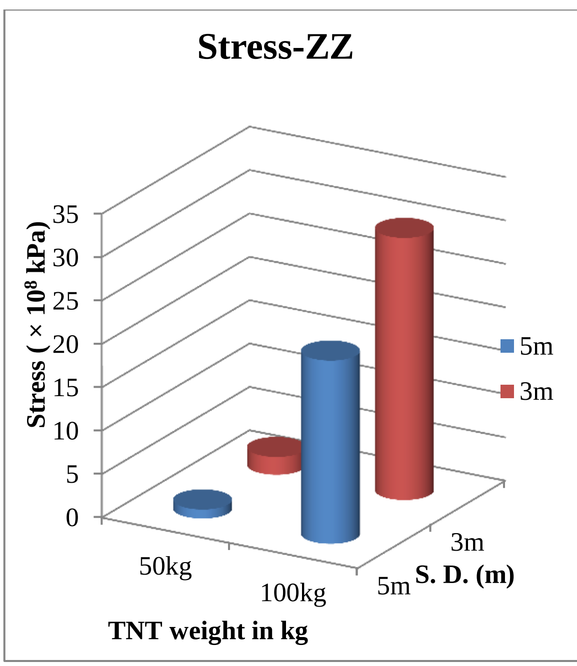

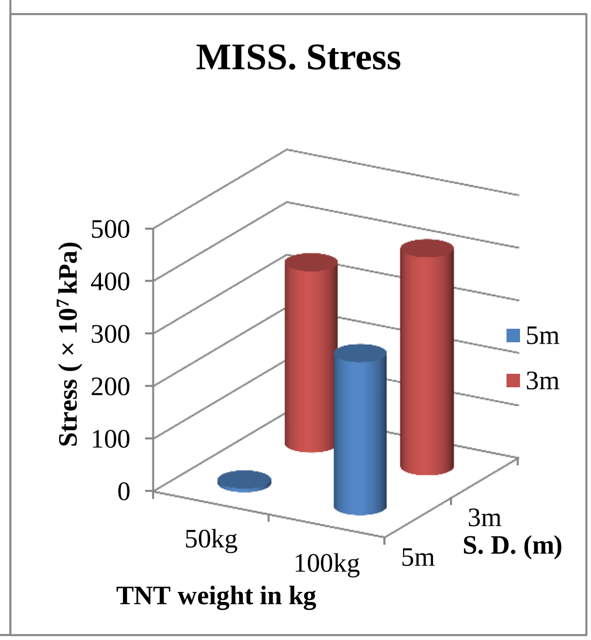

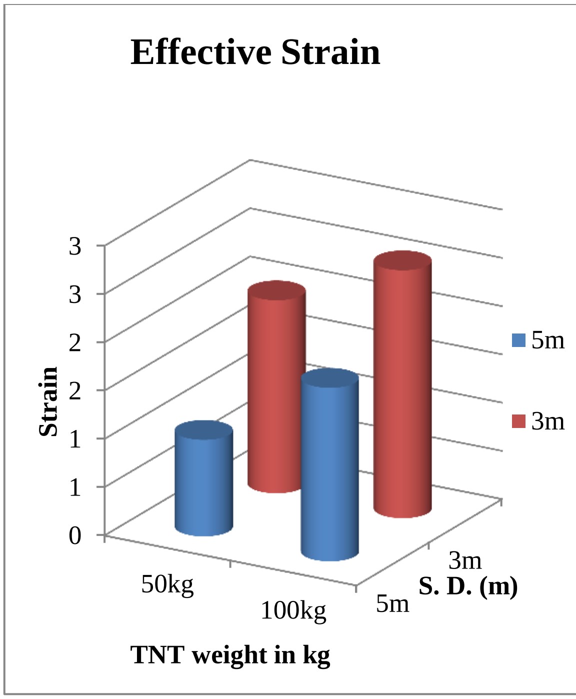
Effective Strain
3
3
2
2
1
1
0
Strain
5m
3m
50kg
100kg
5m
3m
S. D. (m)
TNT weight in kg

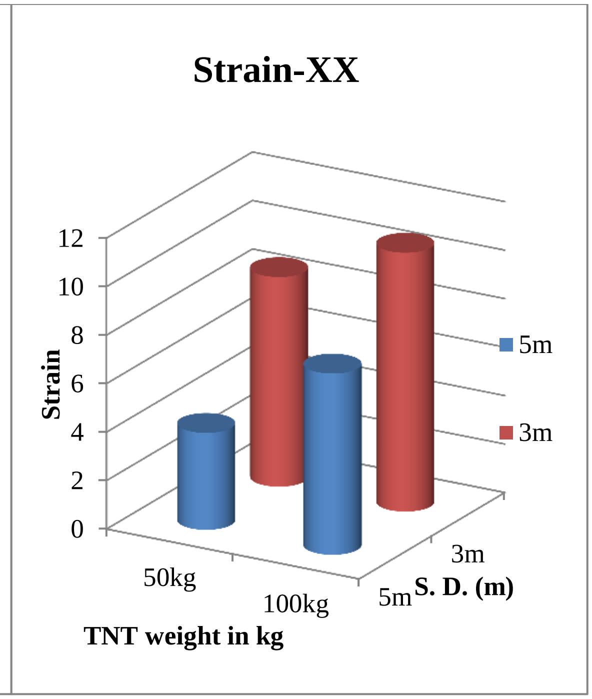
Strain-XX
12
10
8
6
4
2
0
Strain
5m
3m
50kg
100kg
5m
3m
S. D. (m)
TNT weight in kg

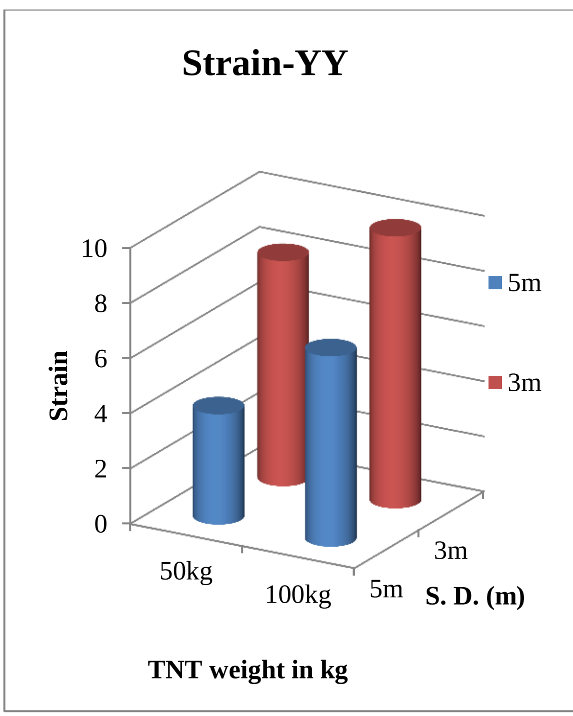
Strain-YY
10
8
6
4
2
0
Strain
5m
3m
50kg
100kg
5m
3m
S. D. (m)
TNT weight in kg

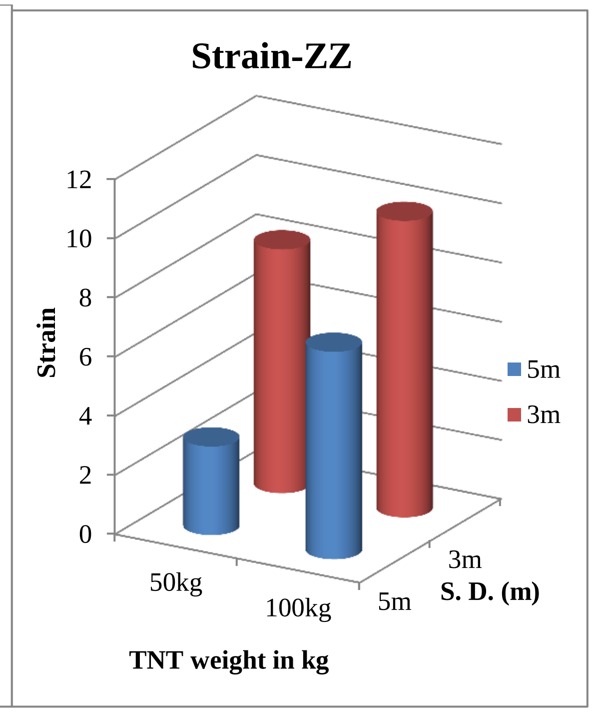
Strain-ZZ
12
10
8
6
4
2
0
Strain
5m
3m
50kg
100kg
5m
3m
S. D. (m)
TNT weight in kg

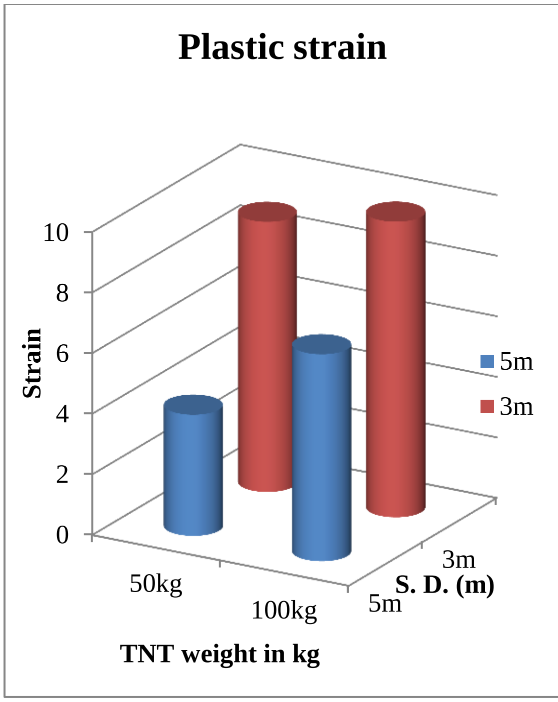
Plastic strain
Strain
10
8
6
4
2
0
50kg
100kg
TNT weight in kg
5m
3m
S. D. (m)
5m
3m

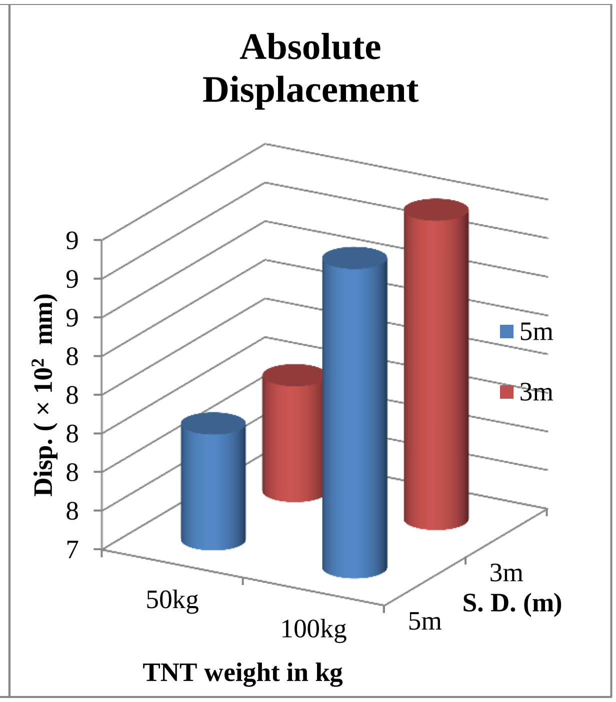
Absolute Displacement
Disp. (× 10² mm)
9
9
9
8
8
8
8
8
7
50kg
100kg
TNT weight in kg
5m
3m
S. D. (m)
5m
3m

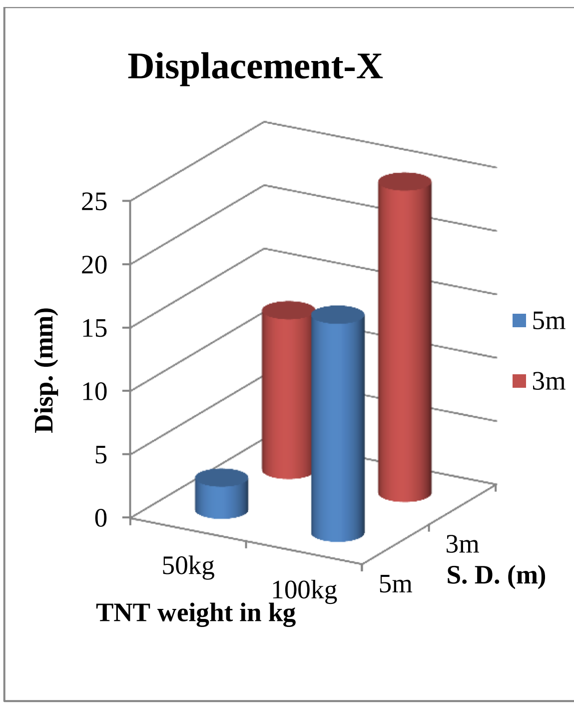
Displacement-X
Disp. (mm)
25
20
15
10
5
0
50kg
100kg
TNT weight in kg
5m
3m
S. D. (m)
5m
3m

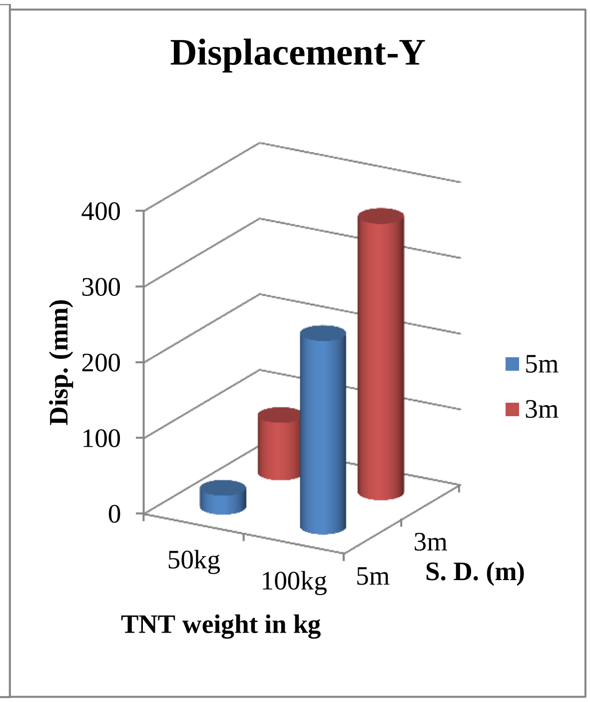
Displacement-Y
Disp. (mm)
400
300
200
100
0
50kg
100kg
TNT weight in kg
5m
3m
S. D. (m)
5m
3m

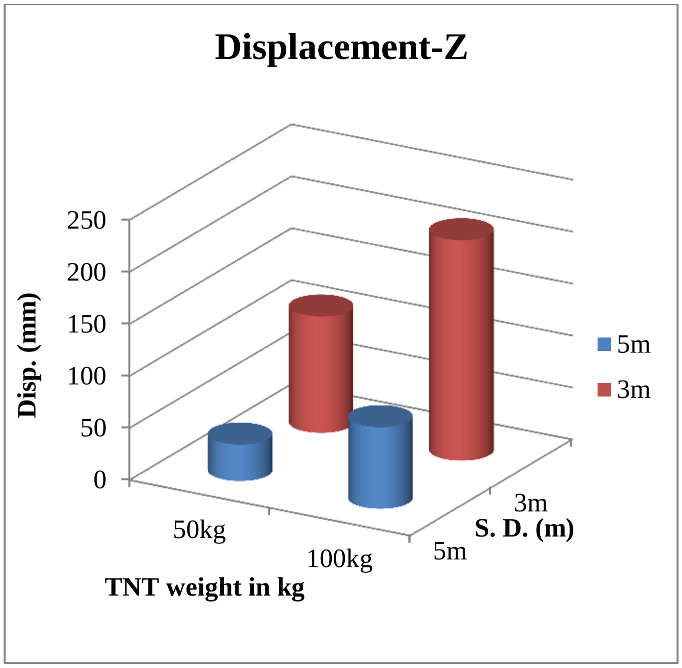

5.3.6 Conclusions drawn from above Plots

- The above plots for different parameters with stand-off distances and TNT weights shows that for 3m Stand-off distance and 100kg TNT weight, every parameter has more value than the corresponding other distances and TNT weights.
- Nearer the point of explosion and greater the TNT weight, more will be the stress or strain or displacement.

5.3.7 Comparison of various properties of different column sections

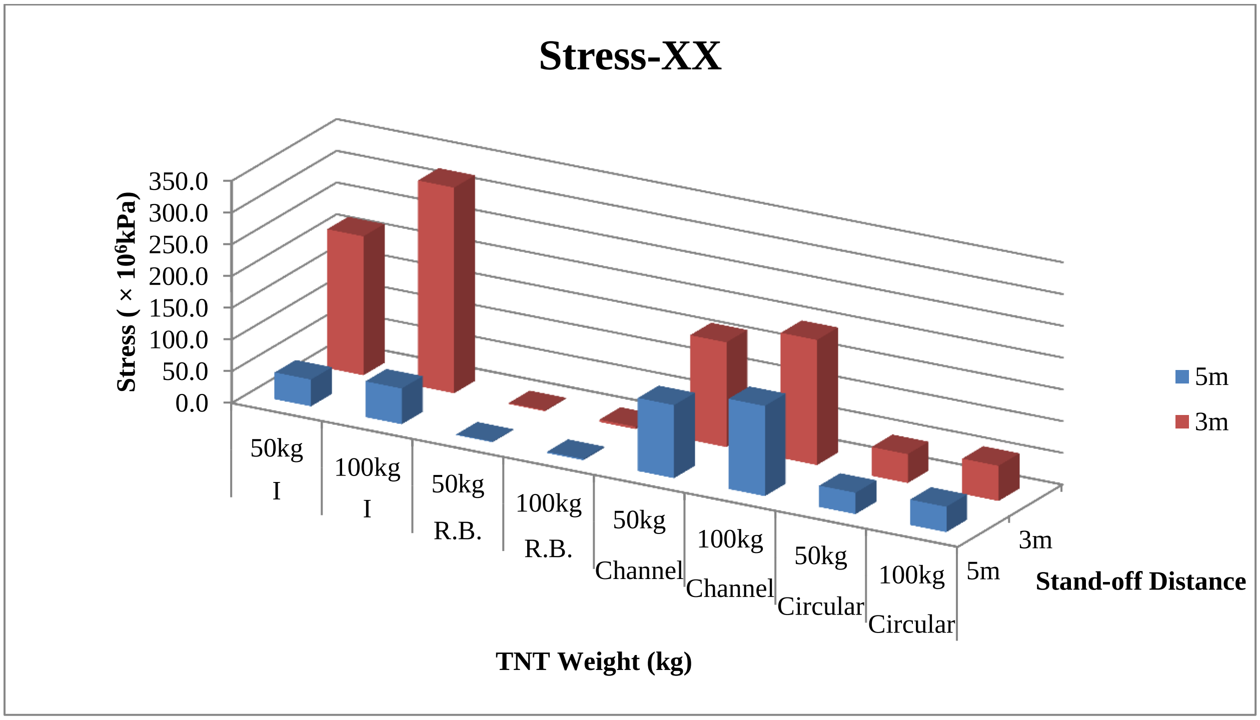

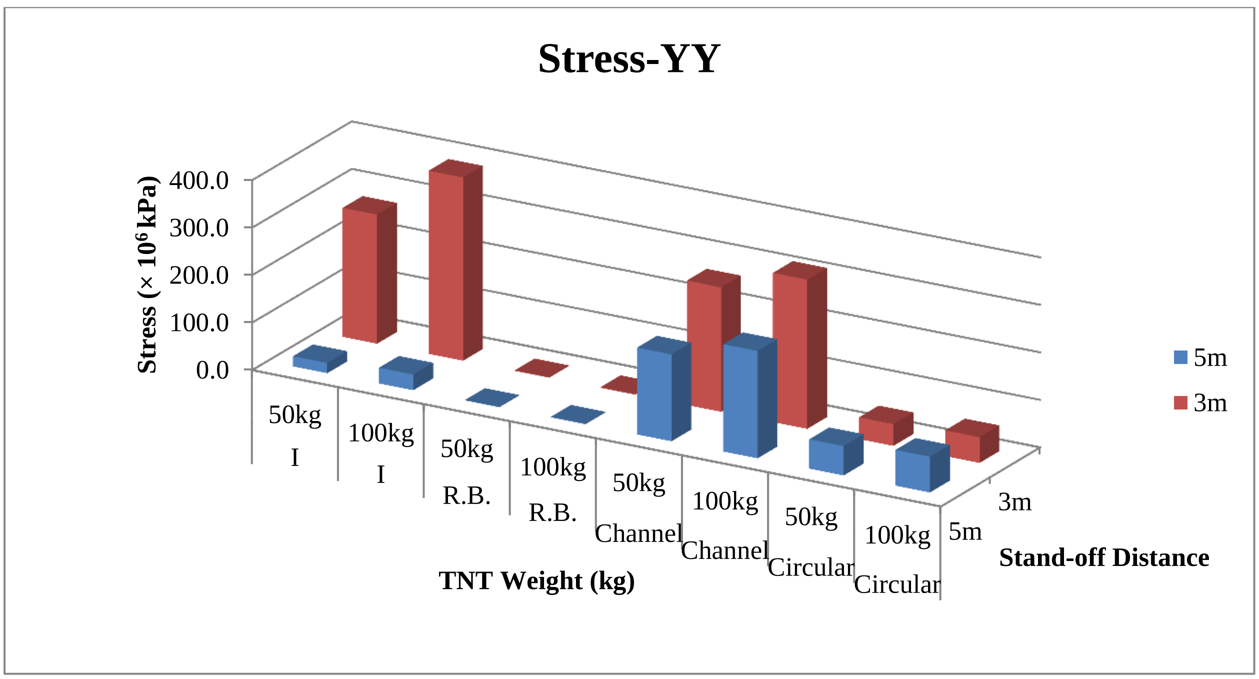

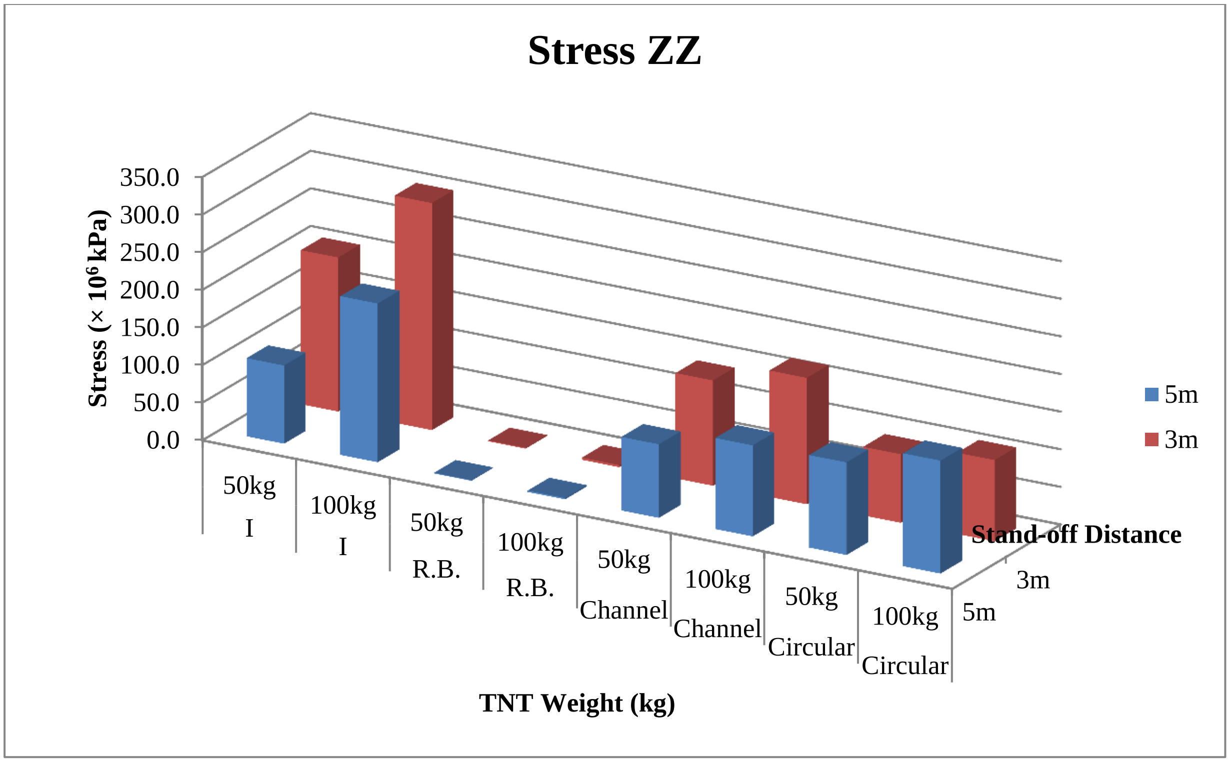
Stress ZZ
350.0
300.0
250.0
200.0
150.0
100.0
50.0
0.0
Stress (× 10⁶ kPa)
50kg I
100kg I
50kg R.B.
100kg R.B.
50kg Channel
100kg Channel
50kg Circular
100kg Circular
TNT Weight (kg)
Stand-off Distance
3m
5m
5m
3m

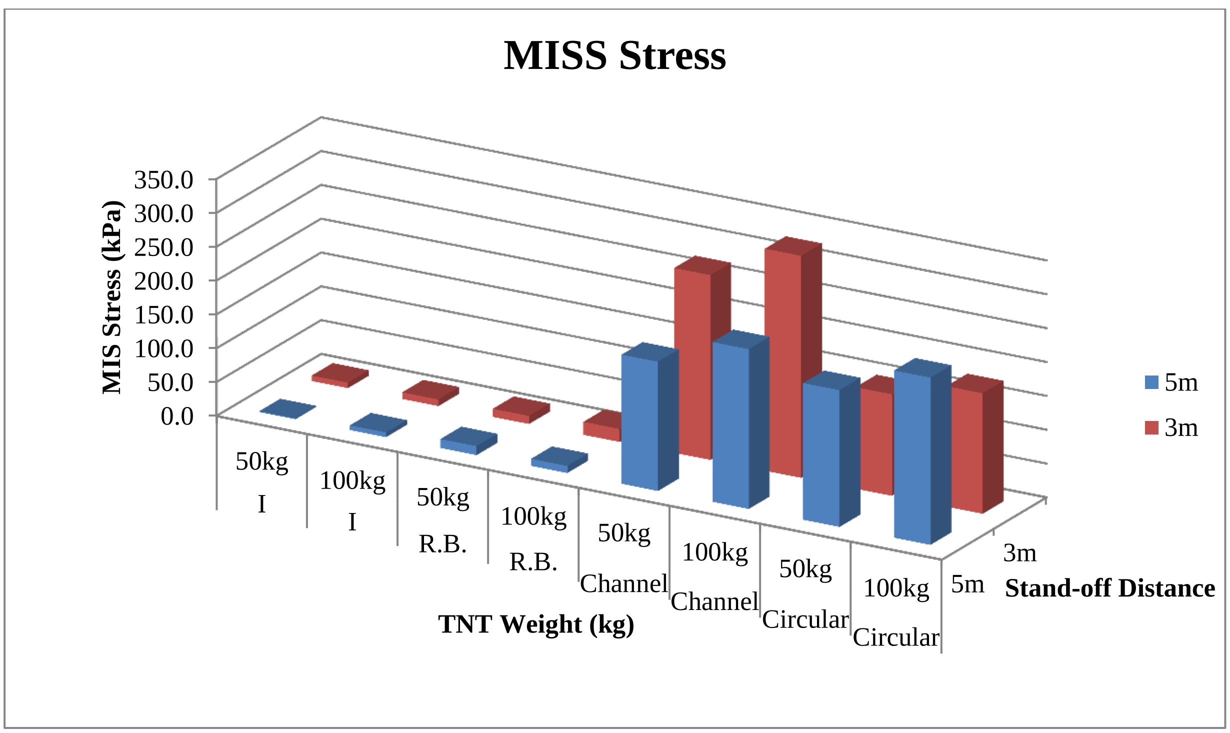
MISS Stress
350.0
300.0
250.0
200.0
150.0
100.0
50.0
0.0
MIS Stress (kPa)
50kg I
100kg I
50kg R.B.
100kg R.B.
50kg Channel
100kg Channel
50kg Circular
100kg Circular
TNT Weight (kg)
3m
5m
Stand-off Distance
5m
3m

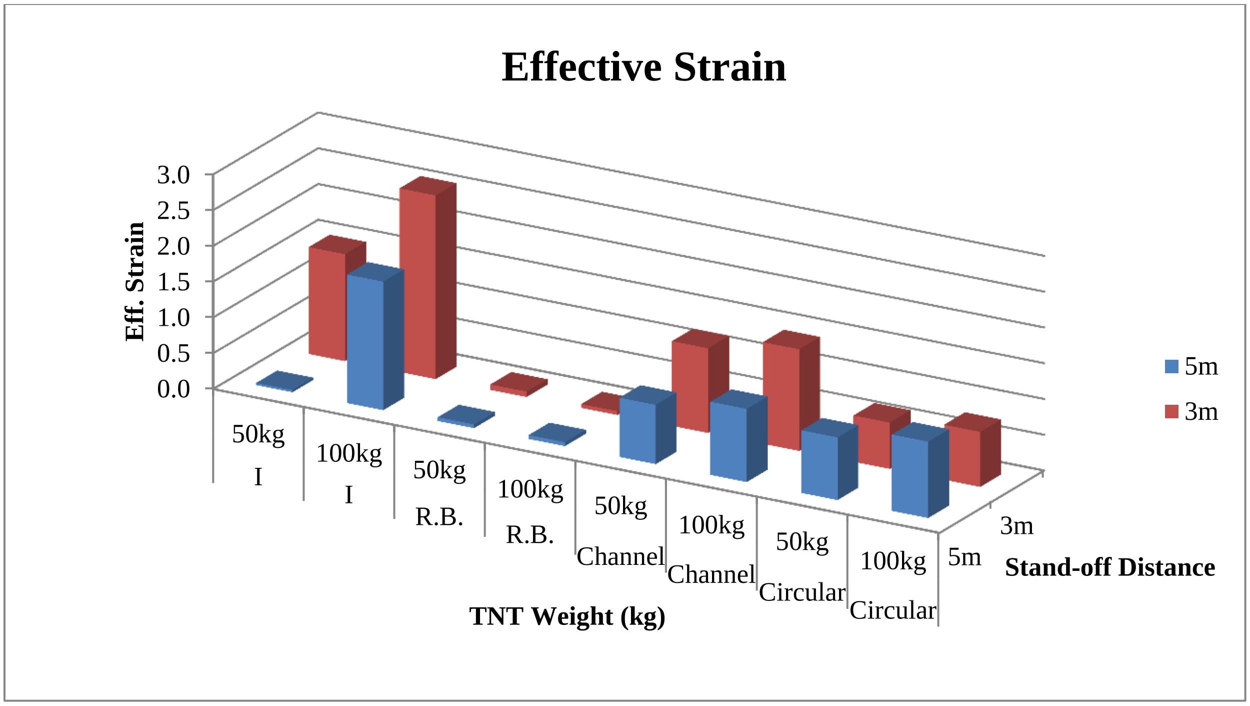
Effective Strain
Eff. Strain
3.0
2.5
2.0
1.5
1.0
0.5
0.0
50kg I
100kg I
50kg R.B.
100kg R.B.
50kg Channel
100kg Channel
50kg Circular
100kg Circular
TNT Weight (kg)
5m
3m
Stand-off Distance
5m
3m

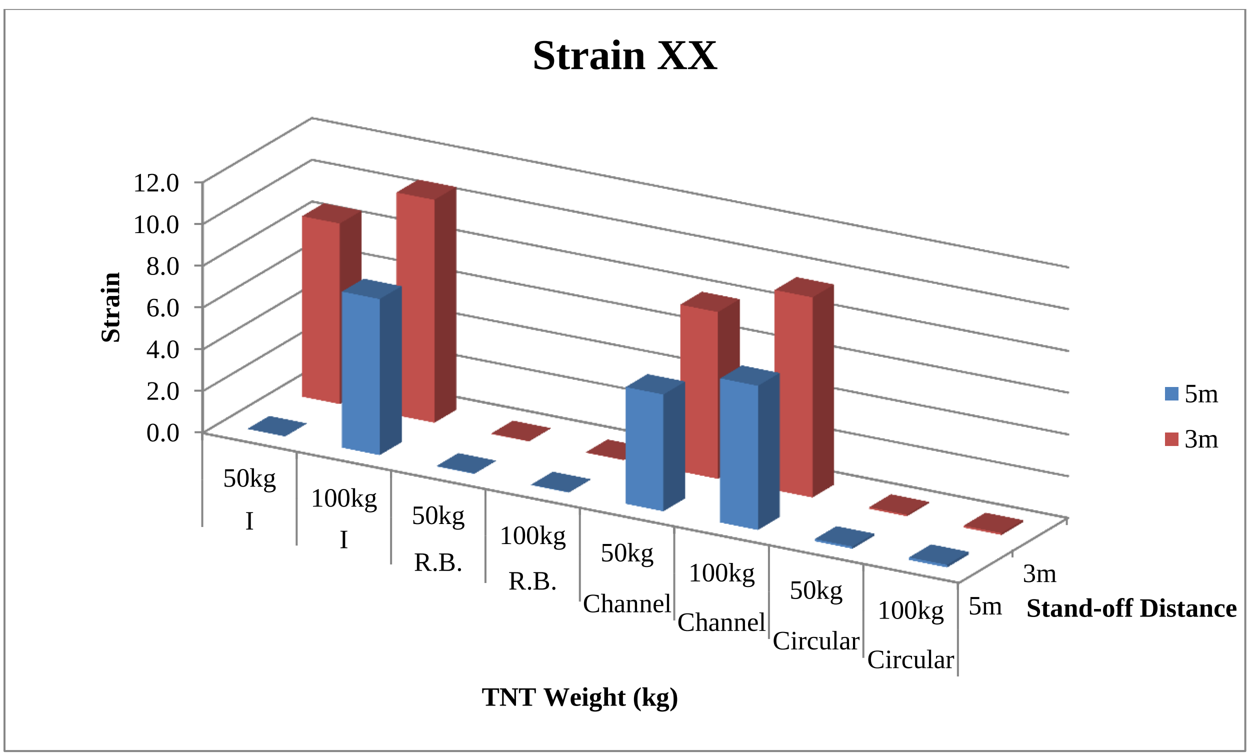
Strain XX
Strain
12.0
10.0
8.0
6.0
4.0
2.0
0.0
50kg I
100kg I
50kg R.B.
100kg R.B.
50kg Channel
100kg Channel
50kg Circular
100kg Circular
TNT Weight (kg)
5m
3m
Stand-off Distance
5m
3m

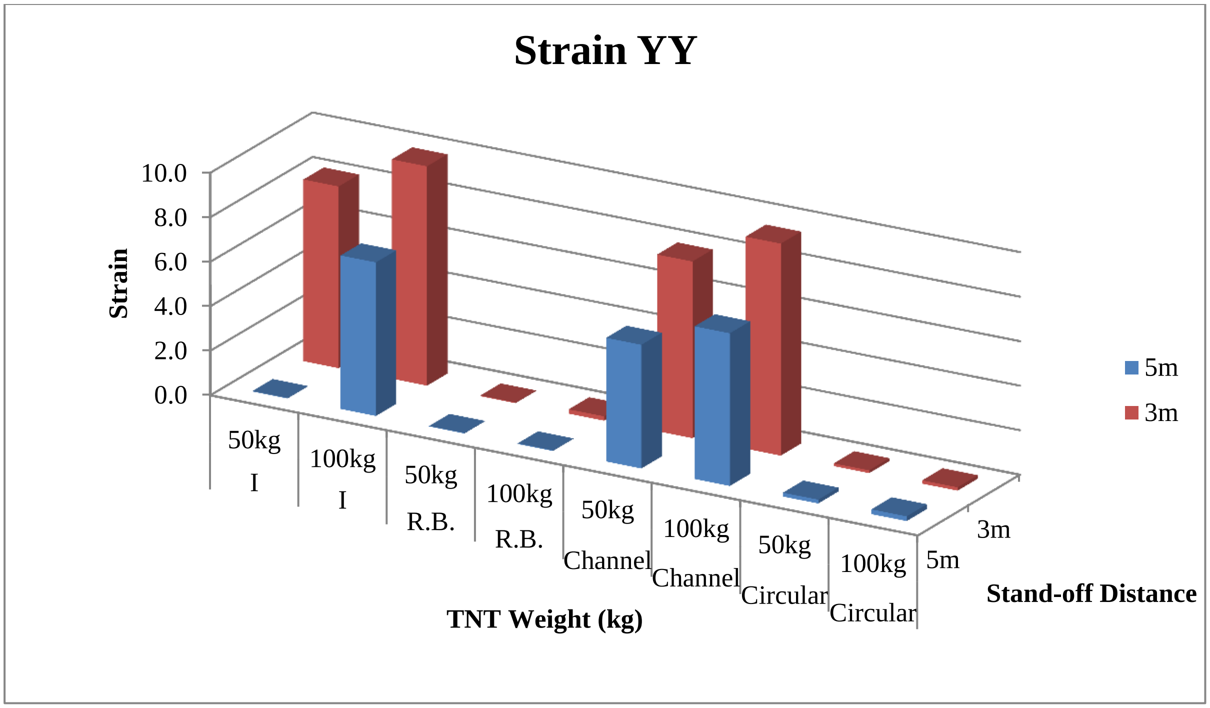
Strain YY
Strain
10.0
8.0
6.0
4.0
2.0
0.0
50kg I
100kg I
50kg R.B.
100kg R.B.
50kg Channel
100kg Channel
50kg Circular
100kg Circular
TNT Weight (kg)
5m
3m
Stand-off Distance
5m
3m

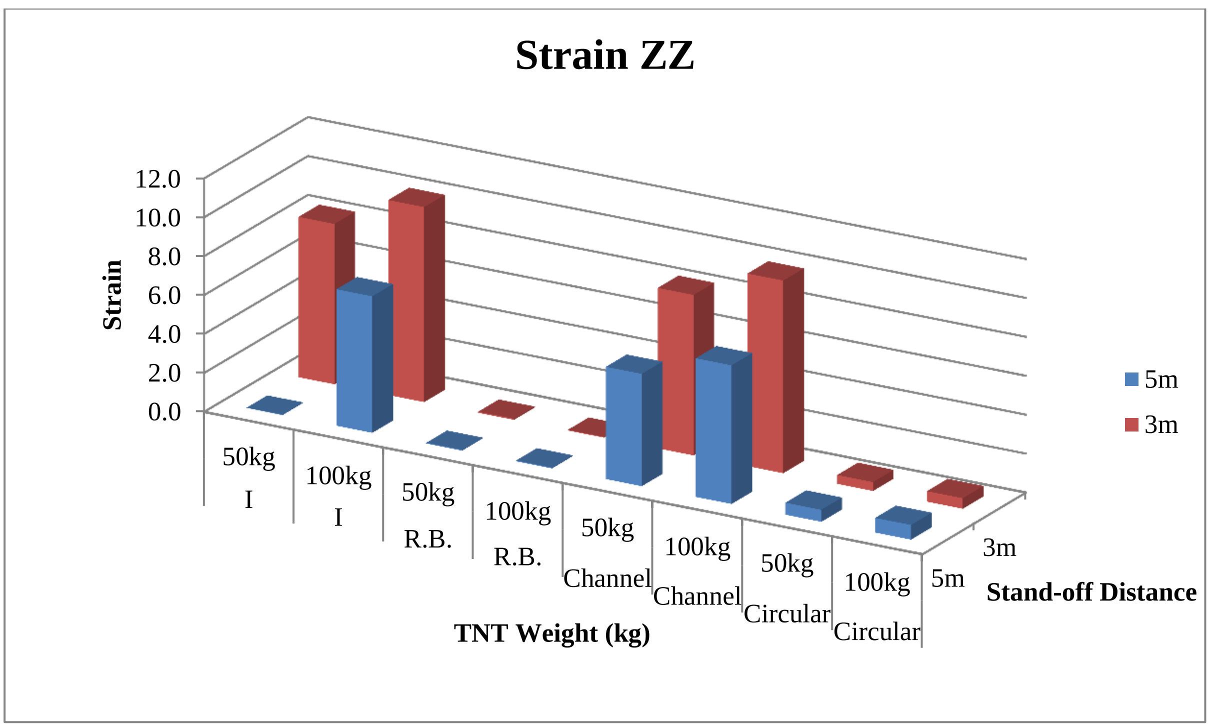
Strain ZZ
Strain
12.0
10.0
8.0
6.0
4.0
2.0
0.0
50kg I
100kg I
50kg R.B.
100kg R.B.
50kg Channel
100kg Channel
50kg Circular
100kg Circular
TNT Weight (kg)
5m
3m
Stand-off Distance
5m
3m

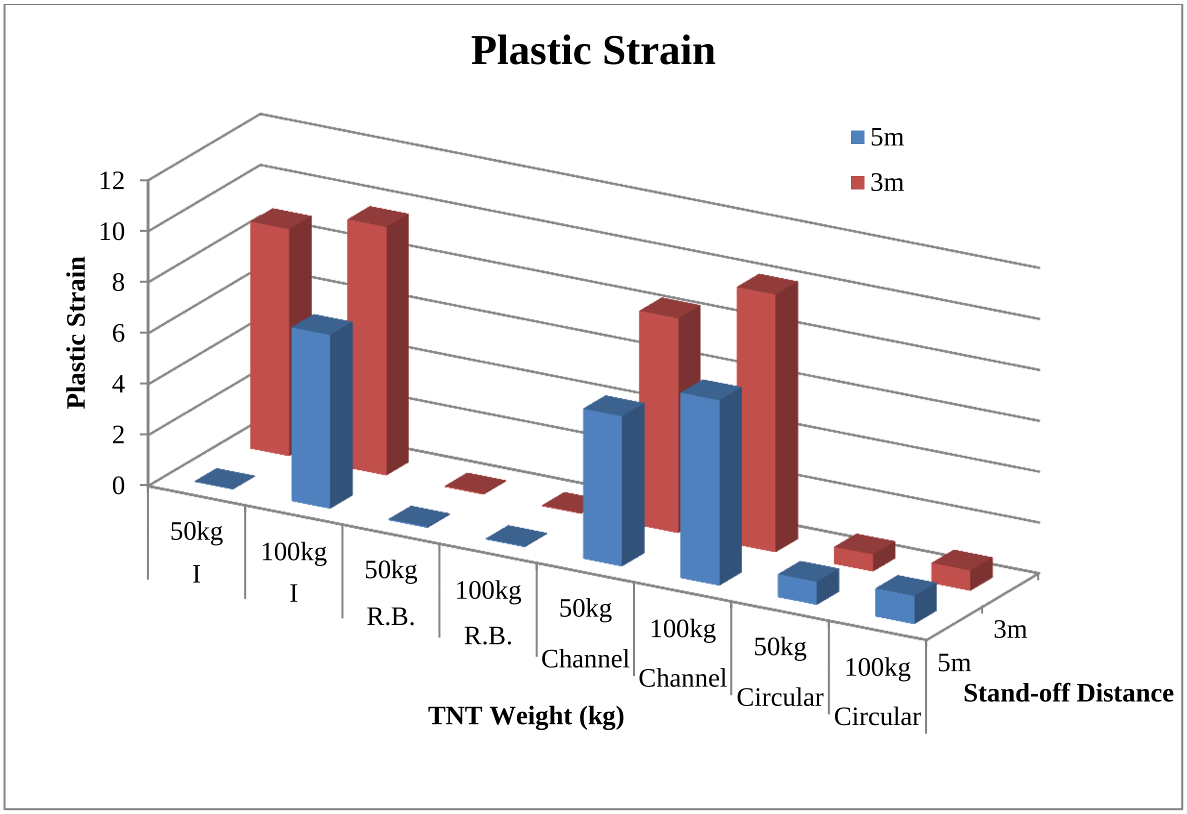
Plastic Strain
5m
3m
12
10
8
6
4
2
0
Plastic Strain
50kg I
100kg I
50kg R.B.
100kg R.B.
50kg Channel
100kg Channel
50kg Circular
100kg Circular
TNT Weight (kg)
3m
5m
Stand-off Distance

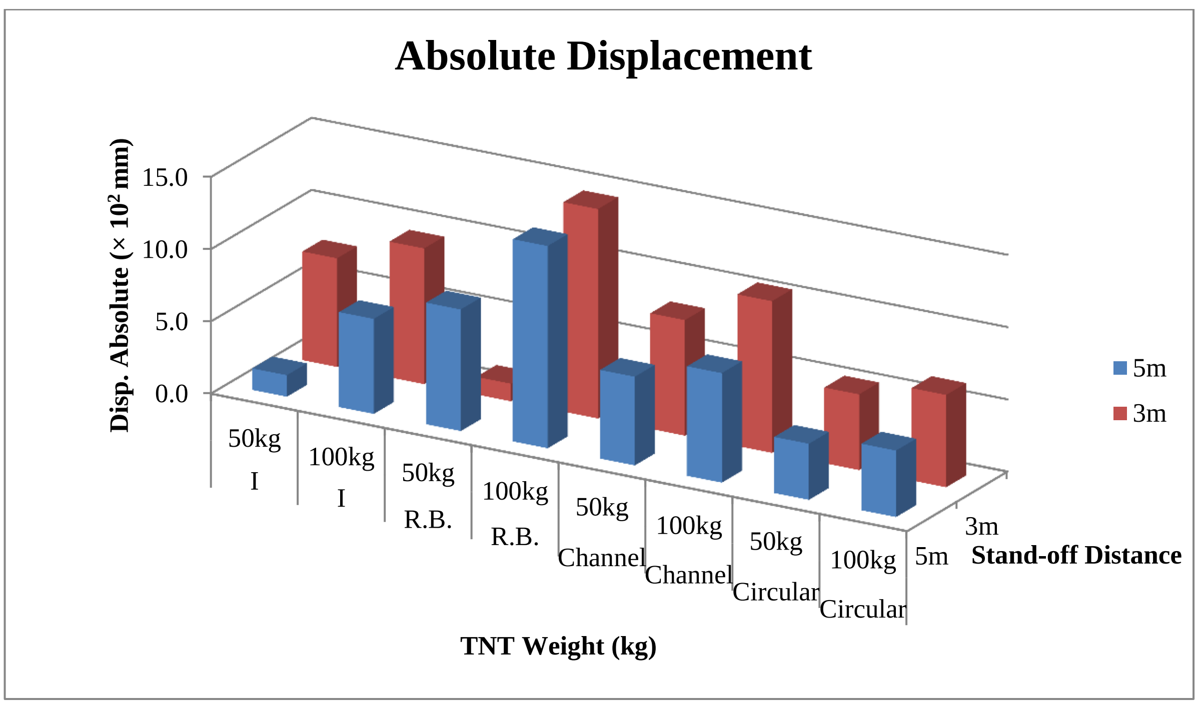
Absolute Displacement
Disp. Absolute (× 10² mm)
15.0
10.0
5.0
0.0
50kg I
100kg I
50kg R.B.
100kg R.B.
50kg Channel
100kg Channel
50kg Circular
100kg Circular
TNT Weight (kg)
3m
5m
Stand-off Distance
5m
3m

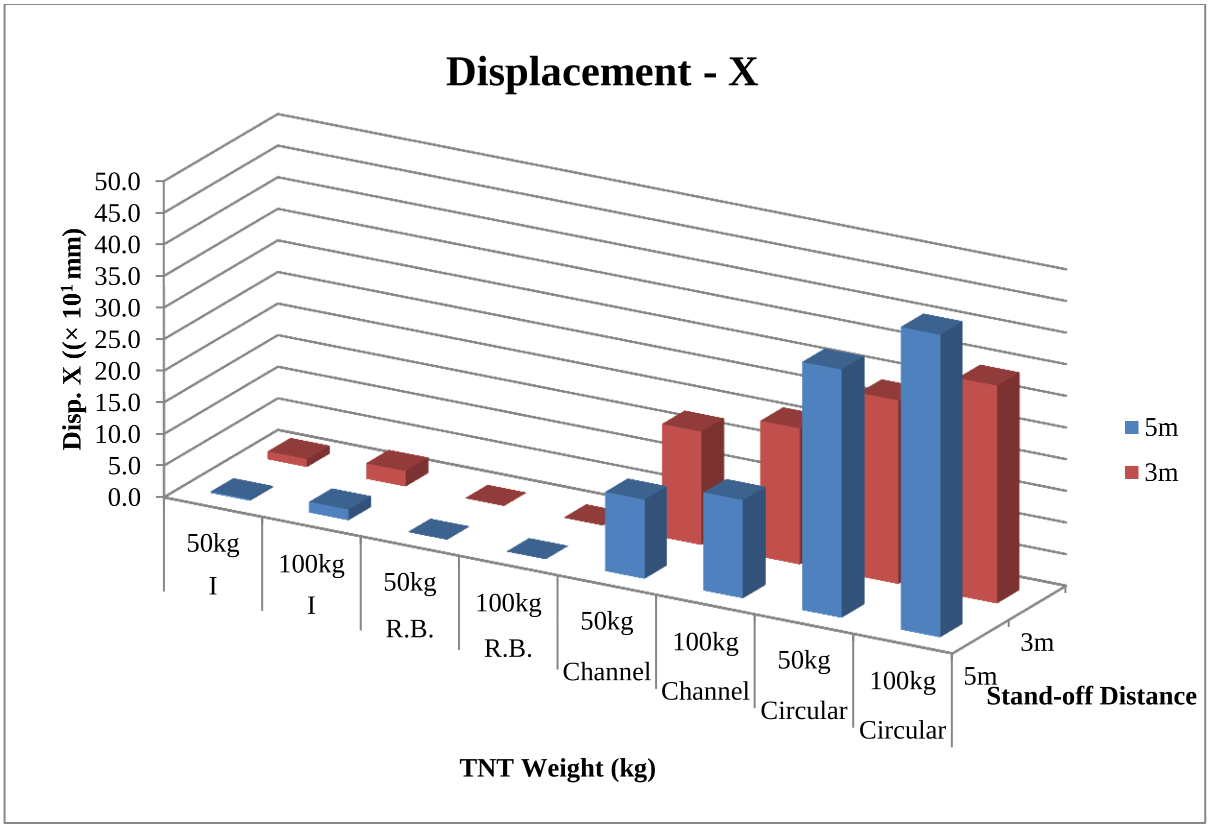
Displacement - X
Disp. X ((× 10¹ mm)
50.0
45.0
40.0
35.0
30.0
25.0
20.0
15.0
10.0
5.0
0.0
50kg I
100kg I
50kg R.B.
100kg R.B.
50kg Channel
100kg Channel
50kg Circular
100kg Circular
TNT Weight (kg)
3m
5m
Stand-off Distance
5m
3m

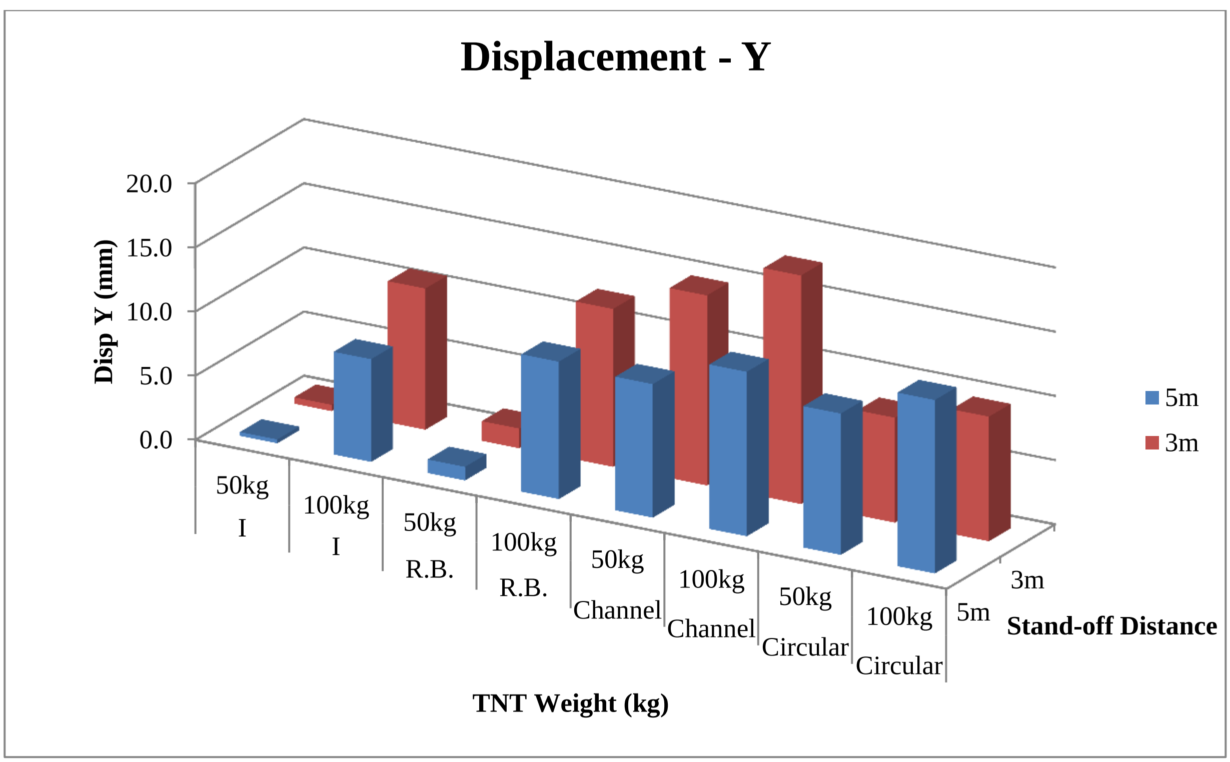
Displacement - Y
Disp Y (mm)
20.0
15.0
10.0
5.0
0.0
50kg I
100kg I
50kg R.B.
100kg R.B.
50kg Channel
100kg Channel
50kg Circular
100kg Circular
TNT Weight (kg)
3m
5m
Stand-off Distance
5m
3m

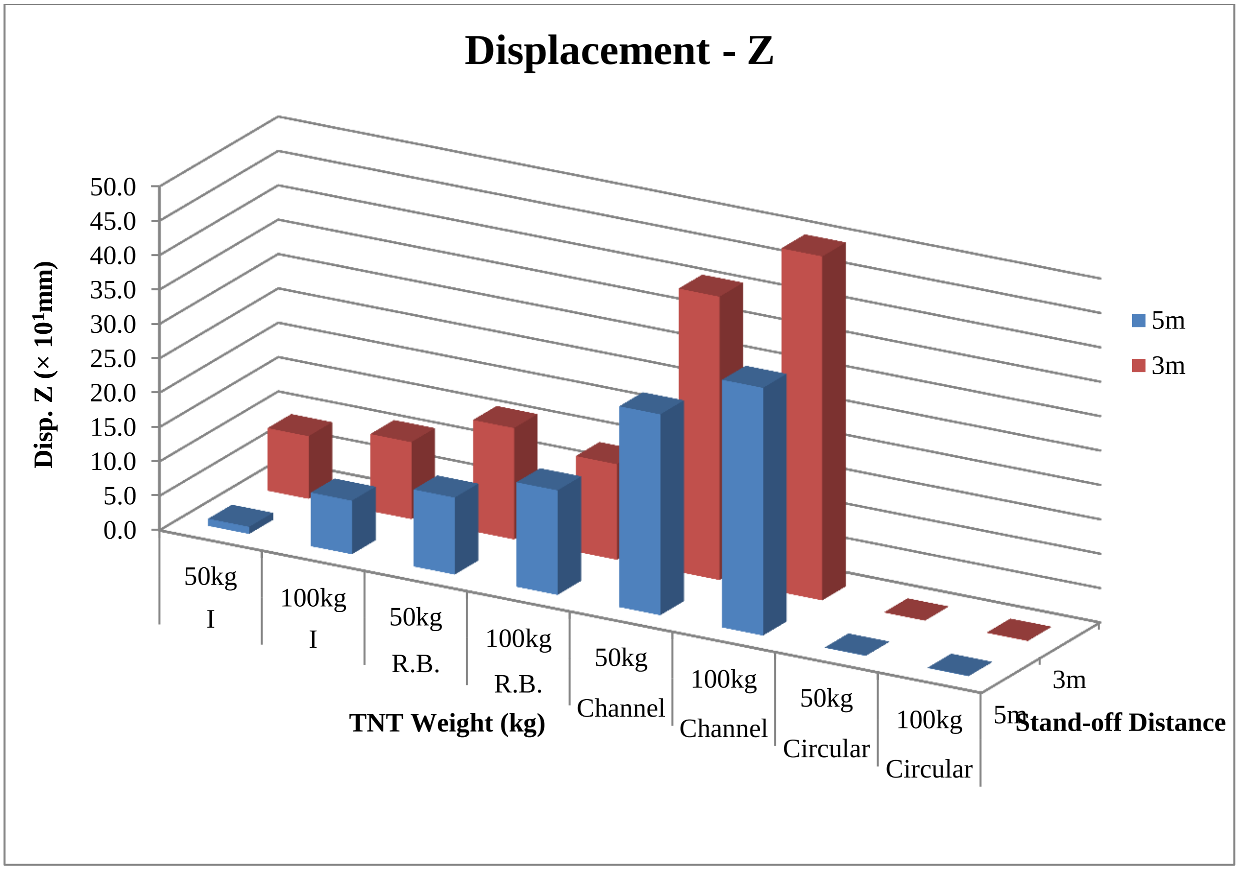

5.3.8 Observations made from the comparison in above cases

- Stresses are maximum on I-section and minimum on Rectangular box section.
- Strains are maximum on I-section and minimum on Rectangular box section.
- Displacements are maximum on channel section and minimum on I-section.
- So we can say that according to stress and strain criterion, rectangular sections behave best while I-sections behave best for displacement criterion.

CHAPTER 6

CONCLUSIONS AND FUTURE SCOPE

6.1 Conclusions

It is observed from literature survey that for the estimation of blast load or pressure, the Empirical approach (Kinney and Graham's) proves to be ideal as blast phenomenon is complex in nature. Complexity arises due to unpredictability of charge weight and standoff distance, the behavior of material under different loading conditions and post blast triggering events. Peak Reflected Pressure is calculated manually by Kinney – Graham Approach and is compared with that comes from Autodyn. A comparative study has been presented for different types of column sections subjected to different TNT weights and stand-off distances.

From the present study, following conclusions are drawn:

- Peak Reflected Pressure calculated by Kinney and Graham approach is slightly more than that computed from Autodyn Analysis on building.
- The percentage of increase in Pressure is between 8% to 17% than that calculated by Autodyn analysis.
- ANSYS Autodyn is an efficient and user friendly tool for simulating explosives and impact loading linking it with workbench environment. The blast simulation was carried out using JWL as equation of state for explosive materials.

- Analysis of column sections in ANSYS Autodyn clearly specifies that effect of explosion largely depends upon the standoff distance and charge weight.
- Pressure will be maximum at first gauge point as it is near most to the blast point.
- For small stand-off distances like 3m, the pressure at gauge points 1& 2 will increase with same rate.
- K.E. is maximum for small stand-off distance and large TNT weights and vice-versa.
- K.E. first increases and then decreases suddenly to zero value when material fails.

- Nearer the point of explosion and greater the TNT weight, more will be the stress or strain or displacement.

- Autodyn Simulation gave good estimate of pressure time history.
- The sections which have been subjected to blast loading signify that pressure will first increase and then decrease with increase in time.
- Stresses are maximum on I-section and minimum on Rectangular box section.
- Strains are maximum on I-section and minimum on Rectangular box section.
- Displacements are maximum on channel section and minimum on I-section.
- So we can say that according to stress and strain criterion, rectangular sections behave best while I-sections behave best for displacement criterion.

- The study presented provides some insight into behavior of the column under blast loads and consequent possibility of progressive collapse of a building.

6.2 Scope for Future Work

The following technical aspects may be considered as a part of further work to the presented report:

1. A group of columns connected with beams directly affected by the blast wave (in 3D) may be considered for modeling in order to better simulate the actual joints stiffness and properties.
2. Advanced high-strain-rate material models may be adopted for assessing the columns' damage to a better accuracy.

REFERENCES

1. Brian R. I., Sezen, H., (2013). “Experimental and analytical progressive collapse assessment of a steel frame building.” *Engineering Structures 56 664–672.*
2. Dewey, M.C., Dewey J.M., (1971), “The properties of the blast waves obtained from the particle trajectories”, *Proc. R. Soc. Lond. A.314, pp. 275-299.*
3. Dharaneepathy M. V. (1995), “Critical distance for blast resistance design”, *computer and structure Vol. 54, No.4.pp.587-595.*
4. Fang F. (2009)., “Progressive collapse analysis of high-rise building with 3-D finite element modelling method.” *Journal of Constructional Steel Research 65- 1269-1278.*
5. Jinkoo. K., Park, J. H., Lee, T. H., (2010). “Sensitivity analysis of steel buildings subjected to column loss.” *Engineering Structures 33 421–432.*
6. Khadid M., Zhou, F.,(2006) “The fully fixed stiffened plates under the effect of blast loads”, *Journal of Structural Engineering, ASCE.*
7. Mark. C. A., Archilla, J. C., (2006). “A Model for Progressive Collapse of Conventional Framed Buildings.” *17th analysis and computation specialty conference.*
8. Mehrdad S., Kazemi, A., Sagiroglu, S., Forest, S. (2011). “Progressive Collapse Resistance of an Actual 11-Story Structure Subjected to Severe Initial Damage.” *Journal of Structural Engineering © ASCE, 893.*
9. Nassar, A. A., Razaqpur, A. G., Tait, M. J., Campidelli, M., Foo, S., (2012). “Strength and stability of steel beam columns under blast load.” *International Journal of Impact Engineering 55 34e48.*
10. Nassar, A. A., Razaqpur, A. G., Tait, M. J., Campidelli, M., Foo, S., (2014). “Dynamic Response of Steel Columns Subjected to Blast Loading.” *ASCE.*
11. Ngo, T., Mendis, P.(2007), “Blast Loads and effects of Blast loads on structures”, *EJSE Special Issue: Loading on structures.*
12. Peirs, J., Verleysen, P., Paepegem, W. V., Degrieck, J., (2011). “Determining the stressestrain behaviour at large strains from high strain rate tensile and shear experiments.” *International Journal of Impact Engineering 38 406e415.*
13. Remennikov M. A., (2003) “A review of methods for predicting bomb blast effects on buildings”, *Journal of battlefield technology, vol 6, no 3. pp 155-161.*
14. Ronald. L. S., (2006), “Response of wide flange steel columns subjected to constant axiai load and lateral blast load”. *Civil Engineering Department, Blacksburg, Virginia.*

15. Stefan S., Krauthammer, T., (2012). "Energy flow in progressive collapse of steel framed buildings." *Engineering Structures 42, 142–153.*
16. Taewan K., Kim, J., Park, J., (2009). "Investigation of Progressive Collapse-Resisting Capability of Steel Moment Frames Using Push-Down Analysis." *journal of Performance of constructed facilities © ASCE, 327.*
17. Tavakoli, H. R., Kiakojouri, F. (2013). **"**Influence of Sudden Column Loss on Dynamic Response of Steel Moment Frames under Blast Loading." *International Journal of Engineering***.**
18. Vlassis, A. G., Izzuddin, B. A., Elghazouli, A. Y., Nethercot, D. A., (2007). "Progressive collapse of multi-storey buildings due to sudden column loss—Part II: Application." , *Engineering Structures, 30, 1424–1438.*
19. Wibowo, H., Lau D.T., (2009). "Seismic Progressive Collapse: Qualitative Point of View." *Civil Engineering Dimension, Vol. 11, No. 1.*
20. Xuemei W., Shi, J., (2013). "Validation of Johnson-Cook plasticity and damage model using impact experiment." *International Journal of Impact Engineering, 60, 67e75.*
21. Young. S. H., Anderson, J. C., (2008)., "Response of a Low Rise Steel Building to Air Blast." *ASCE.*